Homo
J. Comp. Hum. Biol.
Published online April 2025

EarlyAccess-Open Access Article

Evidence of lead poisoning and the co-occurrence of metabolic disease in Archaic/Early Classical (6th–5th century BCE) Laurion, Greece

Anna Lagia[1,2,*], Sydney Patterson[1], Isabelle De Groote[1]

[1] Department of Archaeology, Ghent University, Ghent, Belgium
[2] Present address: Sedanstrasse 30, 79098 Freiburg, Germany
* Corresponding author: annalagia@gmail.com

With 15 figures and 1 table

Abstract: Lead is one of the most toxic heavy metals and environmental pollutants on earth capable of adversely affecting every organ in the human body, with harmful short- and long-term effects. In the Laurion region of southeastern Attica, Greece, the extraction of silver-rich lead ores has been practiced since prehistoric times. This area was heavily mined during the late Archaic and Classical periods significantly contributing to Athens' wealth and sovereignty. Mining and metallurgical activities declined towards late antiquity but resumed in the late 19th century, continuing until the end of the 20th century. Vestiges of these activities still dot the landscape posing potential environmental risks. Although the chemical effects of lead on the human skeleton are well-documented, the osteological imprint of lead contamination, especially in classical antiquity, remains unexplored. This paper examines lesions characteristic of lead poisoning found on the remains of a 2-year-old infant from Laurion dating to the Archaic/Early Classical period (6th–5th century BCE). The study employs non-invasive techniques, including macroscopic analysis, digital microscopy, plain radiography, and micro-CT imaging, to assess the presentation, distribution, pathogenesis, and etiology of the lesions. Anatomical areas formed by endochondral ossification, including the metaphyses of the long bones, the sternal ends of mid-ribs, and the condyle(s) of the mandible, are affected by bone hypertrophy and the formation of lead lines or lead bands. Additionally, hyperplasia of the cranial vault is diagnostic of anemia, while lesions on the endocranial surface indicate encephalopathy, which is associated with high levels of lead exposure and is often fatal. The presence of lesions diagnostic of scurvy and those consistent with rickets further supports the co-occurrence of multiple metabolic diseases in the infant skeleton. The manifestation of these lesions can provide insights into the history of lead toxicity and its lasting effects.

Keywords: metal poisoning; lead toxicity; silver mining; comorbidity; metabolic disease

1 Introduction

Lead, one of the most common heavy metals on the earth's crust, can be very harmful to health (Agency for Toxic Substances and Disease Registry [ATSDR] 2020; U.S. Environmental Protection Agency [EPA] 2022). Numerous studies have highlighted its harmful effects when used in the production of items such as gasoline, batteries, solders, water pipes, paint, ceramic glazes, cosmetics, folk remedies, food packaging, hair dyes, ammunition, toys, and jewelry. It seems to be most harmful in the areas where it is mined, smelted, manufactured and disposed of. Today we are aware of areas around the world where lead levels are very high (Kordas et al. 2018; Global Burden of Disease [GBD] 2019; Risk Factor Collaborators 2020; Zhou et al. 2022). This is largely a result of industrial lead mining and processing activities, as well as areas where lead gasoline and lead-based paint are still used. Both the environment and the people working in these settings face significant health risks and adverse consequences.

There is no organ system in the body that is not affected by lead, as numerous studies on the nervous, endocrine, hematological, renal, cardiovascular, immunological, reproductive, and skeletal systems confirm (ATSDR 2020; Wani et al. 2015). Of particular concern is the nervous system, due to the irreversible impact of lead on children's mental health and behavior (Lanphear et al. 2005; Larsen & Sánchez-Triana 2023). It has been suggested that early lead exposure can lead to adverse effects later in life, including increased aggression and delinquency during adolescence, as well as cardiovascular diseases in adulthood (American Academy of Pediatrics Council on Environmental Health 2016). Lead

DOI: 10.1127/homo/2025/1878
E. Schweizerbart'sche Verlagsbuchhandlung, 70176 Stuttgart, Germany, www.schweizerbart.de

has an even greater impact on children aged 0–5 years, as their rapid development and higher lead absorption rates make them more vulnerable than older children and adults (James & OShaughnessy 2023; Larsen & Sánchez-Triana 2023). This means that the same lead environment will affect infants, children and adults differently and will have different long-term effects on their lives. Before 1986, lead poisoning was defined as having blood levels above 30 μg/dL (Wright et al. 1999). Today, no level of lead in the body is considered safe, as even the lowest blood levels (≤ 5 μg/dL) can cause serious adverse effects (ATSDR 2020, p. 9).

1.1 Pathways of lead toxicity – the effects of lead on metabolism

Lead toxicity can occur through air, water, food, house dust, and soil (Chisolm & Barltrop 1979). It can be ingested, inhaled and, less often, enter the body dermally. Absorption through the gastrointestinal tract is its main route of entry. Young children are particularly vulnerable to this pathway because of their high rate of metabolism that allows higher absorption; behaviors that increase their exposure, such as hand-to-mouth transfer; and a lower stature that brings them closer to inhaling dust from the contaminated soil (von Lindern et al. 2016; Hauptman et al. 2017). Toxicity can also occur during fetal life in case the mother is affected, through lead passing through the placenta as early as 12–14 weeks in utero (Resnick 1995). Prenatal lead toxicity can cause spontaneous abortion, premature birth, low birth weight and reduced growth (American Academy of Pediatrics Council on Environmental Health 2016, p. 4).

Besides the age and physiological state, which includes pregnancy, menopause, or a pathological condition, the absorption of lead is also dependent on the nutritional level of an individual. Periods of fasting and nutritional deficiencies, particularly in calcium, iron and vitamin C, enhance lead absorption (ATSDR 2020, pp. 281–283, 340). Associations between lead level and iron deficiency have been noted in children 0–5 years of age, especially from low socioeconomic groups where, in addition to inadequate nutrition, behaviors such as pica (eating inedible items) and geophagy (eating dirt) may be involved in the development of both conditions (Freeman 1970; Clark et al. 1988; Wright et al. 1999). The relationship between the two conditions may go both ways. Given that lead antagonizes iron, it predisposes to the development of iron deficiency. At the same time iron deficiency predisposes to greater absorption and retention of lead. Both conditions can have a negative effect on overall development with long-term adverse effects in already poverty-stricken environments. Moreover, through enzymatic inhibition of heme biosynthesis and structural changes inducing fragility in the red blood cell membranes, lead can cause hemolytic anemia (Aly et al. 1993; Valentine et al. 1976). Affecting the endocrine system, chronic exposure to lead decreases serum levels of vitamin D starting at levels above 10 μg/dL (ATSDR 2020, p. 118). In children with high lead levels, the production of 1,25-dihydroxyvitamin D, an active vitamin D metabolite crucial for bone mineral metabolism, is inhibited, causing vitamin D levels to drop to those seen in metabolic bone diseases (Rosen et al. 1980; Mahaffey et al. 1982; ATSDR 2020, p. 337).

The mechanisms of lead toxicity are common in all cells and include perturbation of ion homeostasis through the displacement of essential metals, such as calcium, iron, zinc and magnesium, important in biological processes and the function of enzymes and proteins; generation of oxidative stress by increase in reactive oxygen species (ROS) production and antioxidant depletion causing damage to cellular components such as lipids, proteins and DNA; inflammation; perturbations in DNA methylation, mitogenesis; and apoptosis (ATSDR 2020, pp. 262–276).

In advanced stages, lead crosses the blood-brain barrier damaging the endothelium of cerebral vessels, which leads to capillary leak and oedema (Eastman & Tortora 2022). Encephalopathy, a late-stage complication of lead toxicity, occurs when blood lead levels exceed 80–100 μg/dL (Eastman & Tortora 2022; Woolf et al. 1990; Betts et al. 1973). Symptoms at this stage include ataxia, hyperirritability, convulsions, lethargy and altered mental state. If the oedema progresses, it can result in "coma, increased intracranial pressure, and death" (Eastman & Tortora 2022).

1.2 Detection of lead exposure in human bone studies

Numerous studies have utilized chemical and isotopic analysis to measure lead concentrations in archaeological human remains (e.g., Aufderheide et al. 1981, 1985; Schroeder et al. 2013; Millard et al. 2014; Rasmussen et al. 2015; Laffoon et al. 2020; Erel et al. 2021). However, only a few studies have osteologically examined the presence of environmental lead and its effects on the human skeleton. Nakashima et al. (2011) identified lead lines in the remains of members of samurai families from the Edo period in Japan (1603–1867). Radiographic features, such as bone hypertrophy, widened metaphyses, and dense metaphyseal bands and lines, were observed in the long bones of five out of 47 (10.6%) samurai children, complementing chemical analysis (atomic absorption) that showed significantly higher lead concentrations in children than in adults, and in children with bone lesions compared to those without such lesions. In a recent study, Panzer et al. (2022) used CT scans to examine Egyptian child mummies from various time periods housed in European museums. They identified metaphyseal lines in 12 out of 21 mummies but attributed dense metaphyseal bands in the knee bones of only one 7–9 years old boy of the Ptolemaic to Roman period to lead poisoning.

There has been limited discussion on the pathogenesis of lead lines, their differential diagnosis, and the potential for comorbidities. Lewis (2018, pp. 271–273) provides a clear

explanation of the differences in pathogenesis between lead lines and growth recovery lines and points out that "to date, no systematic study of lead lines in the bones of children from archaeological contexts has been carried out" (Lewis 2018, p. 273).

Moore et al. (2021) examined the effects of lead toxicity on metabolic diseases in the Roman Empire by analyzing lead content in tooth enamel (using ICP-MS) and its correlation with conditions like rickets, scurvy, and anemia. They found that children had over twice the lead concentration of adults, suggesting higher childhood lead exposure was linked to lower life expectancy and increased frailty in the Roman Empire. Among non-adults, 71% (46/65) showed lesions consistent with metabolic diseases, while only 29% (15/51) of adults had similar lesions. Children with metabolic disease lesions had significantly higher lead levels, indicating a strong link between lead exposure and childhood health during this period.

In Greece, lead exploitation dates to prehistoric times. In the Laurion region (Fig. 1), mining related to silver metallurgy began at the end of the Neolithic period and continued into modern times. Systematic and rescue excavations in this area have uncovered an extensive network of mines and metallurgical workshops dedicated to silver extraction (Mussche et al. 1973; Conophagos 1980; Salliora-Oikonomakou 1985; Mussche 1998; Kakavoyannis 2001; Docter & Webster 2018; Kapetanios 2023). During the Classical period, the discovery of a new mining vein led to a surge in lead extraction, which significantly enhanced the wealth and influence of the Athenian city-state in the 5th century BCE.

In this paper, using both macroscopic and radiographic methods we analyze bone lesions in the remains of a non-adult from the Thorikos West Necropolis at Laurion who lived during the Archaic/Early Classical period. The skeleton exhibits widespread lesions, some suggesting lead exposure, while others point to metabolic disease. After introducing the site, we present the bone lesions and explore differential diagnoses. This study is the first bioarchaeological research to address the diagnosis of such lesions and the co-occurrence of metabolic disease in classical Greece.

Fig. 1. The region of Laurion in Southeast Attica (ellipse) with the site of Thorikos (rectangle). Adapted from *Thorikos: A Mining Town in Ancient Attika* (p. 93), by H. Mussche 1998, Belgian Archaeological School in Greece. Copyright 1998 by the Belgian School at Athens.

2 Material and methods

2.1 The region of Laurion in SE Attica

The region of Laurion spans a vast geographical area in southeastern Attica (Fig. 1) densely populated with mines, quarries, metallurgical workshops, farmsteads, harbors and cemeteries (Apostolopoulos & Kapetanios 2021). Silver in the Laurion region was extracted from lead ores (galena) found in various geological layers (Skarpelis & Argyraki 2009; Voudouris et al. 2021; Ross et al. 2021). The extraction of galena began with surface layers and, from the 5th century BCE onward, extended to deeper deposits as richer veins were discovered. This led to the establishment of an industrial environment that continues to influence the area today. Although the peak of mining activity occurred in the 4th century BCE, it continued into the 3rd century BCE and Late Antiquity through renewed mining and the reprocessing of old slags. It has been estimated that 1.4 million tons of lead and 3500 tons of silver were produced in the area from prehistoric times to the 1st century BCE (Conophagos 1980). In the late 19th and early 20th centuries, intensive remining, coupled with residues from past lead processing, significantly increased environmental contamination, effects of which are still evident today. Environmental and population studies have shown substantial lead contamination in plants, animals, and both adult and juvenile populations in the region (Nakos 1979; Nakou et al. 1980; Nakou 1985; Maravelias et al. 1989, 1994, 1998; Demetriades et al. 2008).

2.1.1 The site of Thorikos

Thorikos was one of the ten demes (political and physical entities) of Laurion, which were part of the city-state of Athens encompassing the entire region of Attica (Apostolopoulos & Kapetanios 2021, p. 437). The deme incorporated a large area, including the Adami plain, the edge of the Potami valley, the Aghios Nikolaos peninsula, and the Velatouri hill, on which the city of Thorikos was established (Mussche 1998, p. 1). The Belgian School at Athens began excavations of the Thorikos site in 1963 and uncovered various contexts, including urban, domestic, industrial, ritual, and mortuary (Mussche 1998; Docter & Webster 2018). The excavations highlighted the significance of mining throughout Thorikos' extensive occupation from the Final Neolithic (ca. 3200 BCE) (Laffineur 2010, p. 26) to several metallurgical workshops in the Classical Period (4th century BCE) (Mussche 1998, pp. 62–63), followed by shorter and smaller re-occupations up to the 8th century CE; in the 19th century CE mining operations were renewed (Mussche 1998, p. 2). The predominance of mining within the Lavreotiki was because galena, a silver-rich lead ore, was abundant making the region integral to the production of silver and other metals (Conophagos 1980). Inscriptions concerning the leasing and operation of Laurion's mines, including Thorikos, were found in the Athenian Agora and demonstrate Athens' interest in exploiting the region's mineral resources (Crosby 1950; Mussche 1998, p. 4). Such demands on an exploitative mining industry would have impacted the physical landscape and the people living within the region (Xenophon, Mem. I, 6, 12.; Nriagu 1983, p. 312; Mussche 1998, p. 2).

Grave 23 was excavated in 1964 in the West Necropolis (sector C52 j4 in Fig. 2), the largest mortuary area (about 153 graves) excavated at Thorikos, dating from the Geometric to the Classical periods (Mussche 1998, pp. 22–29; Bergemann 2021). Minimal information was recorded during this grave's excavation, and it has yet to be fully described in publications (Bingen 1967a, p. 33, n. 1; Bingen 1969, p. 101). What can be discerned, primarily through excavation photos (Fig. 3), is that this was a funerary pithos (height: 50+ cm) laid on its side into a stone-lined pit, within the ruins of an earlier 9th century BCE room (Bingen 1967a, pp. 33–34).

The field journal noted that the vessel was missing fragments towards the topsoil (and any possible covering), potentially due to intensive looting nearby (Bingen 1967b, p. 42). The vessel's mouth was closed with a large square stone slab and no grave artefacts were found inside with the fragmentary skeleton, or outside of the vessel. Initially, the grave was broadly dated to between the 9th and 5th century BCE structures of the West Necropolis; it was later suggested that this grave probably dates to the 6th–5th century BCE (Bingen 1967a, p. 33, n1; Bingen 1969, pp. 100–101).

2.2 The human remains

The human remains from Grave 23 of the Thorikos West Necropolis (abbreviated in this paper as Tho-23) are in a moderate state of preservation, with several bones missing or fragmented (Fig. 4). Many postmortem fractures are old, indicating that some of the bone damage occurred within the burial environment. The remains were originally misidentified as those from an adult cremation (Bingen 1967a, p. 33, n.1), but it is now clear that they belong to the inhumation of a non-adult. The altered morphology of the left femur confirms the identification of the remains with the documented excavation finds (Fig. 3b). There is no evidence from the excavation records of articulated or anatomically arranged bones. The disturbance may have resulted from the above-mentioned looting. Although the remains have been studied in the past (Defever 1990), research has only recently focused on pathologies.

Preserved are the diaphyses of many long bones, parts of the cranial vault, facial bons, and cranial base, a portion of the right hemimandible, two teeth, rib fragments, the right ilium, and a metatarsal. Most bones retain their cortical surfaces and shape, facilitating the examination of pathological lesions. Several bones were covered with encrustations that required specialized cleaning to remove.

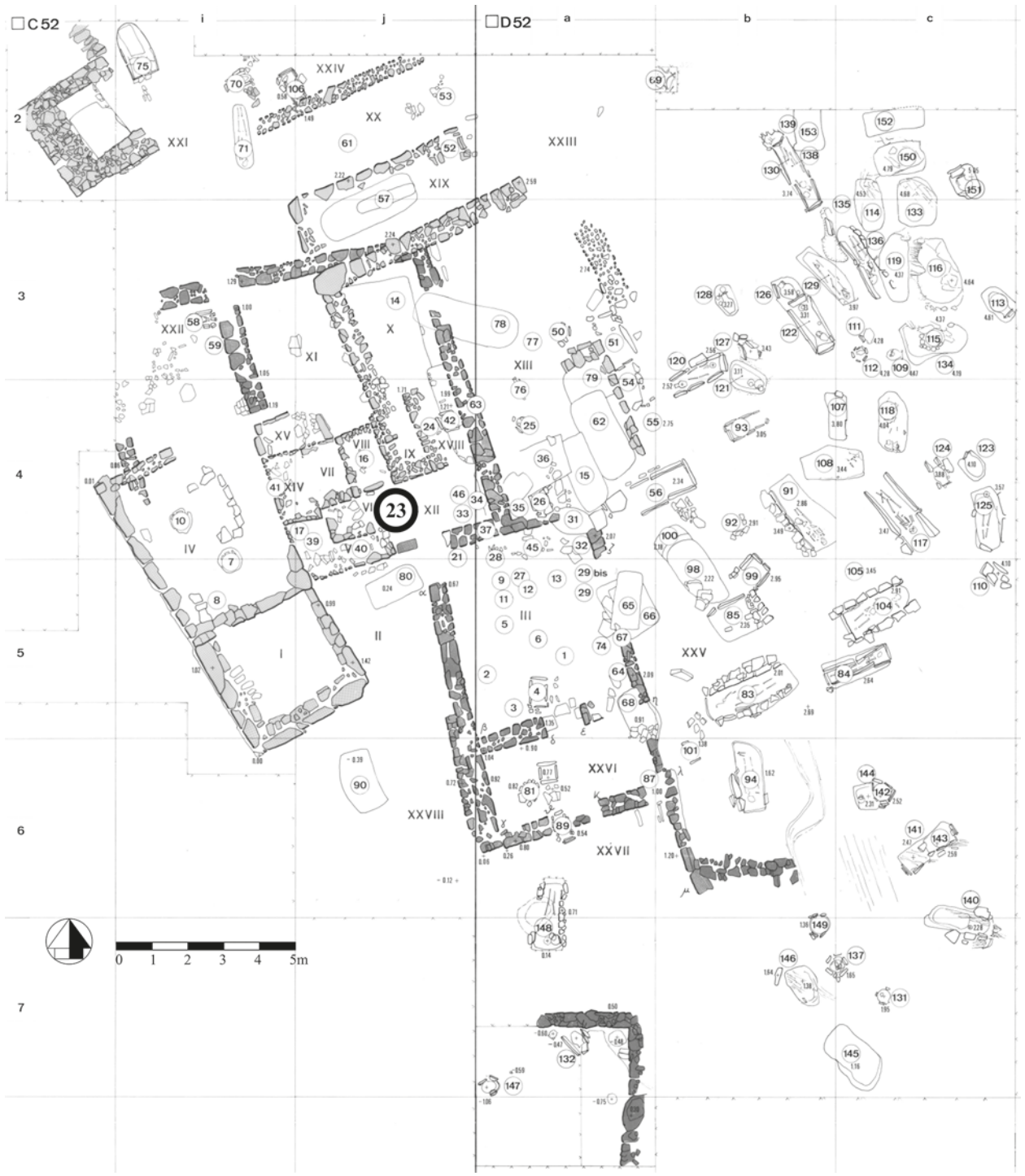

Fig. 2. Location of grave 23 in the Thorikos West necropolis. Adapted from archived version of excavation map by M. Mouraux 1972.

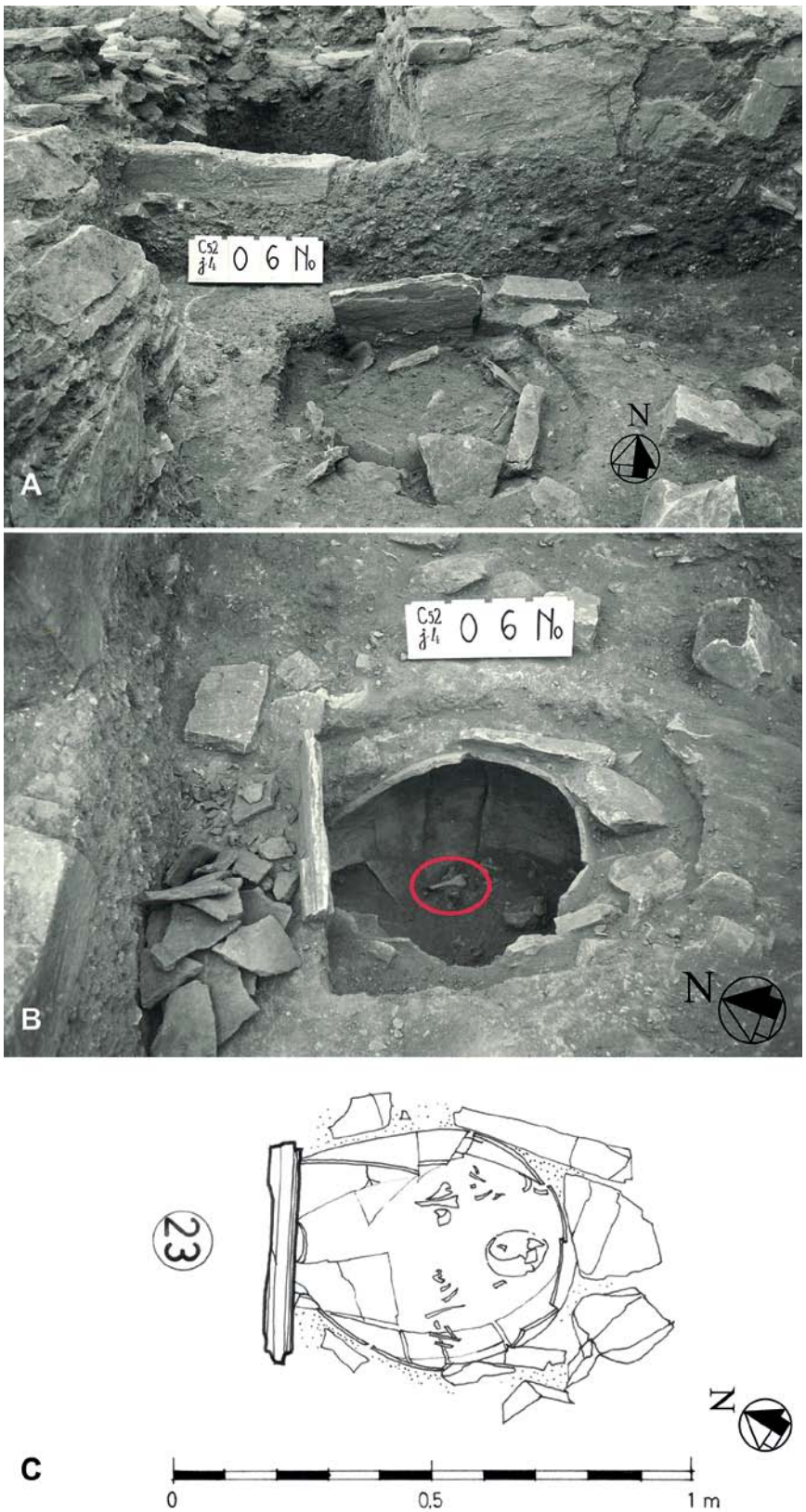

Fig. 3. Pithos 23 in situ before **(A)** and after **(B)** removal of the infill. Circled in (B) is the distal half of the left femur with the characteristic flaring of the distal metaphysis. **(C)** Diagrammatic representation of the human remains in the interior of the pithos. Adapted from archived excavation photographs and drawings. Copyright 2024 by TARP.

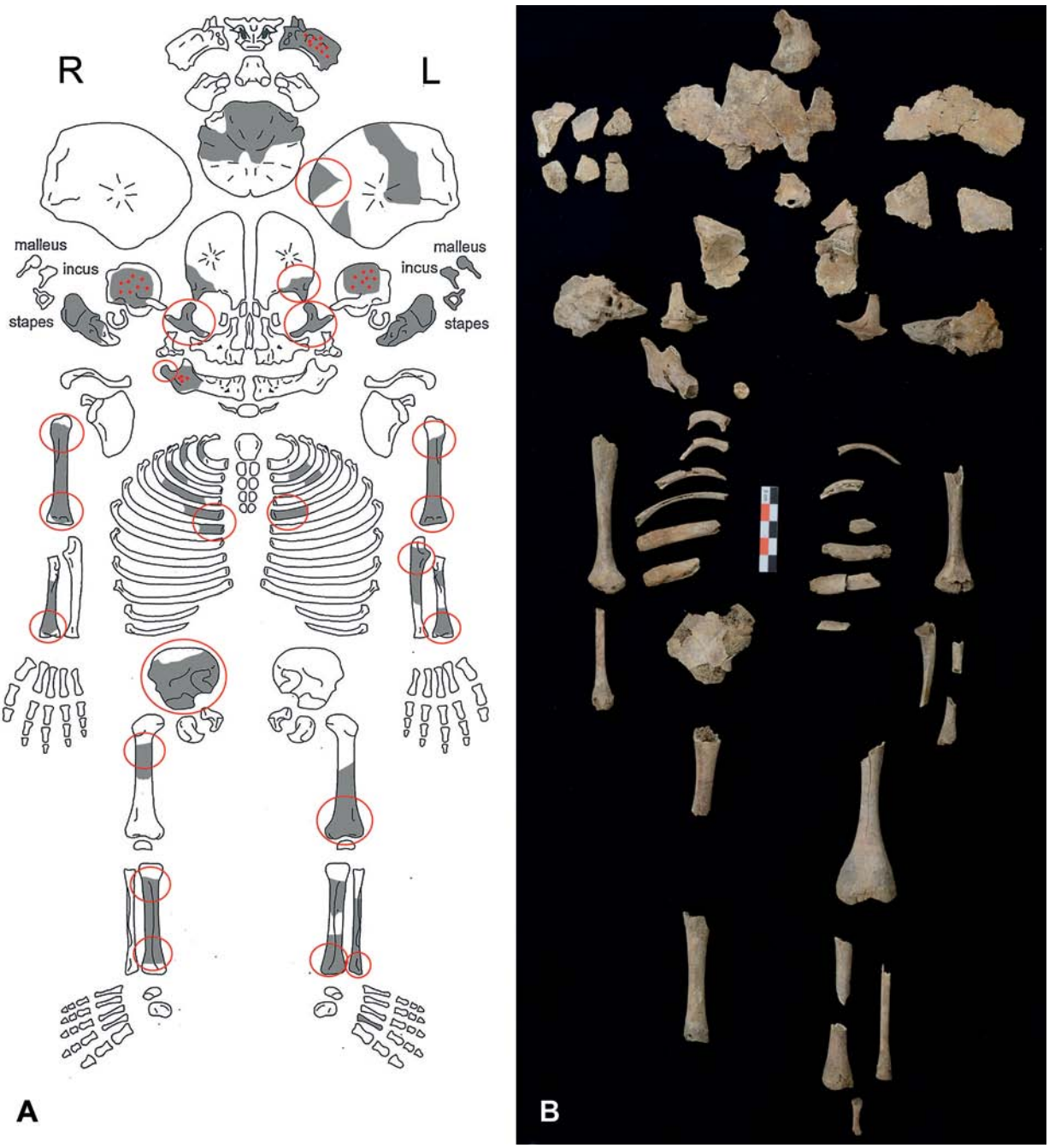

Fig. 4. **(A)** Schematic and **(B)** photographic inventory of the skeletal remains. The pathological areas are marked with ellipses; dots designate lesions on the endocranium and the medial surface of the mandible. Credit for Visual Template: Pascal Adalian, CNRS Université de la Mediterranée, UMR 6578; adopted by Lisa Steige.

2.3 Methods

The estimation of the age-at-death was determined based on the fusion stage of primary ossification centers (Cunningham et al. 2016), dental development (Moorrees et al. 1963; AlQahtani et al. 2010), and the approximate length of the long bone diaphyses (Cardoso et al. 2014; Cunningham et al. 2016; Maresh 1955). Sex estimation was not attempted due to the young age of the individual. Macroscopic, digital microscopic (Dino Lite 2.0), and radiographic (MinXray 750) analyses were performed at the Wiener Laboratory of the American School of Classical Studies in Athens to evaluate pathological lesion expression, distribution, and for differential diagnosis. An industrial micro-CT scanner, BRUKER Skyscan 1273 was used to produce a micro-CT scan of the left femur and right radius (kV = 100; uA = 150). This resulted in a 102.81 µm resolution. The reconstructed file was segmented using Amira 5 in the ArcheOs laboratory at the University of Ghent, Belgium.

3 Results

The human remains from Thorikos Pithos 23 belong to an infant estimated to be around 2 years old. There appears to be a small discrepancy between the age-at-death estimated from the teeth (1.5–2.5 years) and the length of the long bones (1.0–1.5 years), suggesting developmental delay. Pathological lesions are observed on both the cranial and postcranial skeleton, impacting the cortical surfaces, diploe, and spongy bone, and altering their shape. Fig. 4A shows the distribution of these lesions across the skeleton. The description of the pathological lesions is organized anatomically, beginning with the cranium and progressing to the ribs, ilium, and long bones.

3.1 The cranium

Fragments of the vault and some facial bones are preserved. Various bone lesions are observed on the ectocranial and endocranial surfaces of these fragments, as well as in the diploe.

Frontal: The diploe of the frontal bone superior to the orbital roof is widened (hyperplastic). The orientation of the trabeculae is not altered (Fig. 5A). The inner table is substantially thicker compared to the outer table suggesting atrophy of the latter. The fragmented bone allows the calculation of the ratio of compact to diploic bone and this is ca. 1:4, far exceeding the 1:2.5 that is considered the cut off point for the identification of marrow hyperplasia (Brickley 2024, p. 100, table 3). Although the fragment from which the measurement is taken is not at the midline as suggested by Brickley (2024), the ratio of compact to diploic bone is too large to be considered normal.

Parietals: A parietal fragment exhibits hyperplasia of the diploe, with a second bone layer forming over the original cortex, creating the appearance of vertical striations in the new bone (Fig. 5B). Notably, the upper diploic layer has large intertrabecular spaces. There is no porosity observed on the ectocranial surface of this fragment.

However, another parietal fragment, which does not show signs of diploic hyperplasia, displays focal porosity on its ectocranial surface. Other traits on the cranium include fine vascular impressions on the outer table of a parietal fragment and irregular bone formation on the endocranial surface of the squamous part of the temporal bones (Fig. 6) and the left lateral of the occipital.

Other traits on the cranium include lesions on the sphenoid and the zygomatic bones. New bone formation is present around the foramen rotundum of the left part of the sphenoid bone (Fig. 7A). The right part of the sphenoid is not preserved. Both zygomatic bones display thickening and porosities smaller than 1 mm in diameter that penetrate the cortex on the anterior, lateral, and posterior surfaces (Fig. 7B).

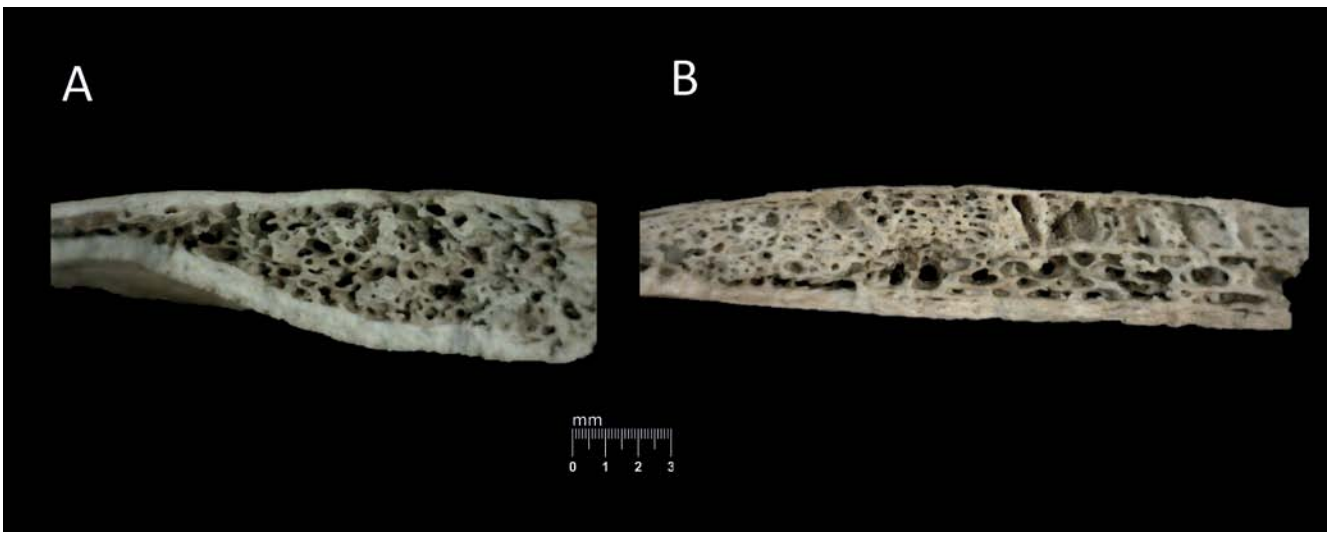

Fig. 5. **(A)** Thickening of the diploe of a frontal fragment superior to the orbital roof (located on the left side of the image). **(B)** Hyperplasia of the diploe of a parietal fragment: a second layer of bone was laid over the cortex of the earlier bone. Note also the large intertrabecular spaces present. In both figures, the outer cranial table is at the top and the inner table at the bottom. Viewed with digital microscopy.

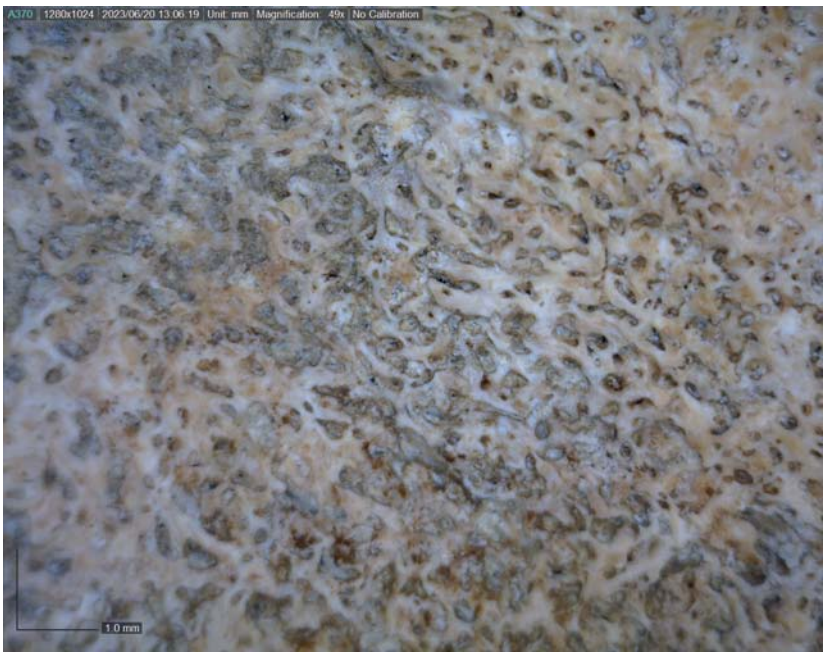

Fig. 6. Irregular bone formation on the endocranial surface of the squamous part of the right temporal viewed with digital microscopy.

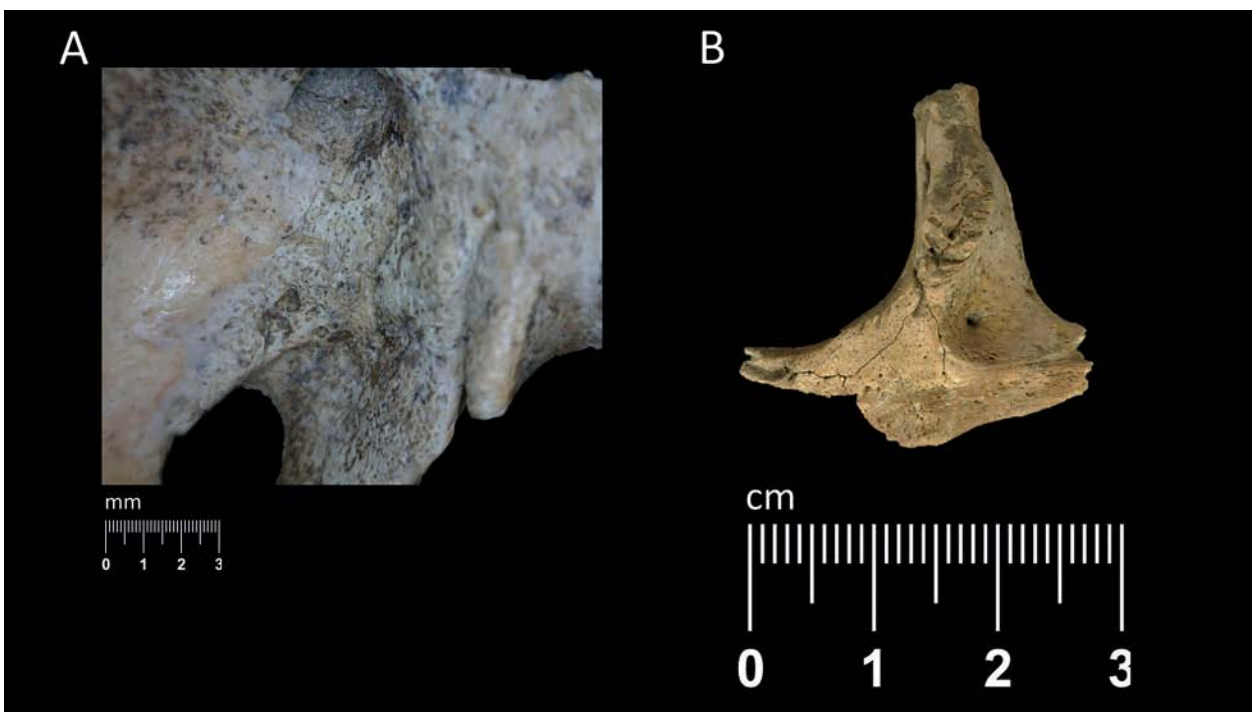

Fig. 7. (A) Bone formation around the foramen rotundum of the left sphenoid. **(B)** Porosity on the posterior and lateral cortical surfaces of the right zygomatic bone.

3.2 The mandible

Two kinds of lesions are observed macroscopically and radiographically on the preserved part of the right hemimandible:

On the medial side of the mandible, beneath the coronoid process abnormal cortical porosity is present (arrow in Fig. 8A).

Moreover, the mandibular condyle is hypertrophic, and its shape is altered (Fig. 8A and 8C). This deformation becomes more apparent when the affected condyle is compared to a normal bone from another individual of similar age-at-death (Fig. 8D). Radiographically the hypertrophic area appears opaque while the trabeculae are accentuated (coarse) throughout (Fig. 8B). Although intrusive soil likely contributes to the increased radiopacity, bone hypertrophy also seems to play a role.

3.3 The ribs

Fragments of the shafts and sternal ends of several ribs are preserved. The sternal ends of several mid-ribs are hypertrophic. The area affected extends shaftwards approximately 20 mm from the sternal end (Fig. 9A). The hypertrophy is directed towards the pleural side of the ribs sparing the outer cortex. Radiographically the hypertrophic area appears opaque (Fig. 9B). Porosity on the pleural side of the affected area likely enabled soil to seep into the bone, increasing radiopacity.

3.4 The right ilium

Only the right ilium is preserved. Depositions of new bone and fine porosity are observed on the visceral surface (Fig. 10A). The radiographic image reveals three radiopaque lines following the contour of the iliac crest, along with accentuated trabeculae throughout the ilium (Fig. 10B).

3.5 The long bones

Multiple lesions are observed in the long bones, including widened metaphyses (flaring), transverse radiopaque lines in the metaphyseal region, dense metaphyseal bands near the growth plate, and accentuated (coarsened) trabeculae. While not all lesions are present in every long bone, at least two appear in each. The widened metaphyses and coarse trabeculae are consistently found in all long bones. The distal metaphyses of the left femur and right radius exhibit the most characteristic combination of these lesions and are further examined by micro-CT imaging to investigate the underlying pathogenesis. Because of incomplete skeletal preservation, it is not possible to determine their presence in the proximal humeri, distal ulnae, proximal radii, proximal tibiae, and proximal fibulae.

The distribution of lesions in the preserved long bones is as follows:

Accentuated (coarse) trabeculae in all bones preserved.

Widened metaphyses (flaring) are present in all respective areas preserved, i.e., the proximal and distal humeri

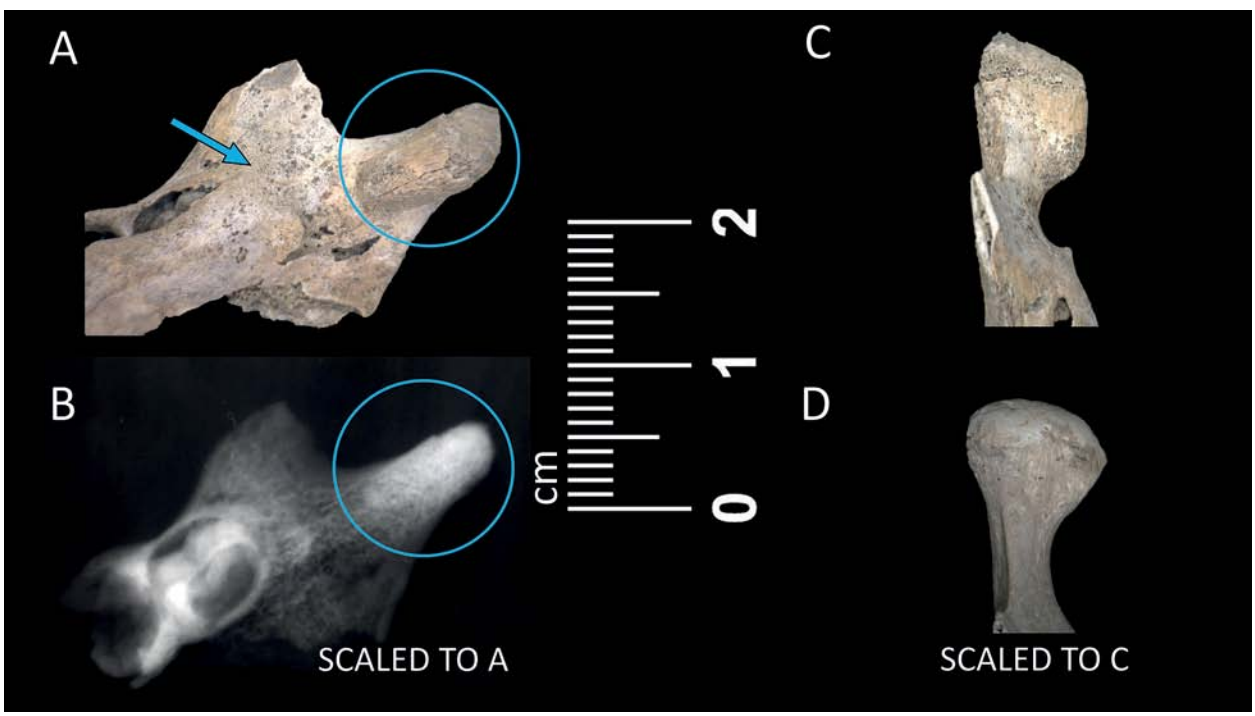

Fig. 8. Right hemimandible. **(A)** Hypertrophic mandibular right condyle (in circle) and abnormal porosity medially below the coronoid process (arrow). **(B)** Radiography displaying radiodensity of the hypertrophic area (in circle) and the stage of formation of the first permanent molar. **(C)** Close-up of the hypertrophic condyle viewed anteriorly. **(D)** The non-pathological mandibular condyle of an infant of similar age-at-death. Photographic images with digital microscopy.

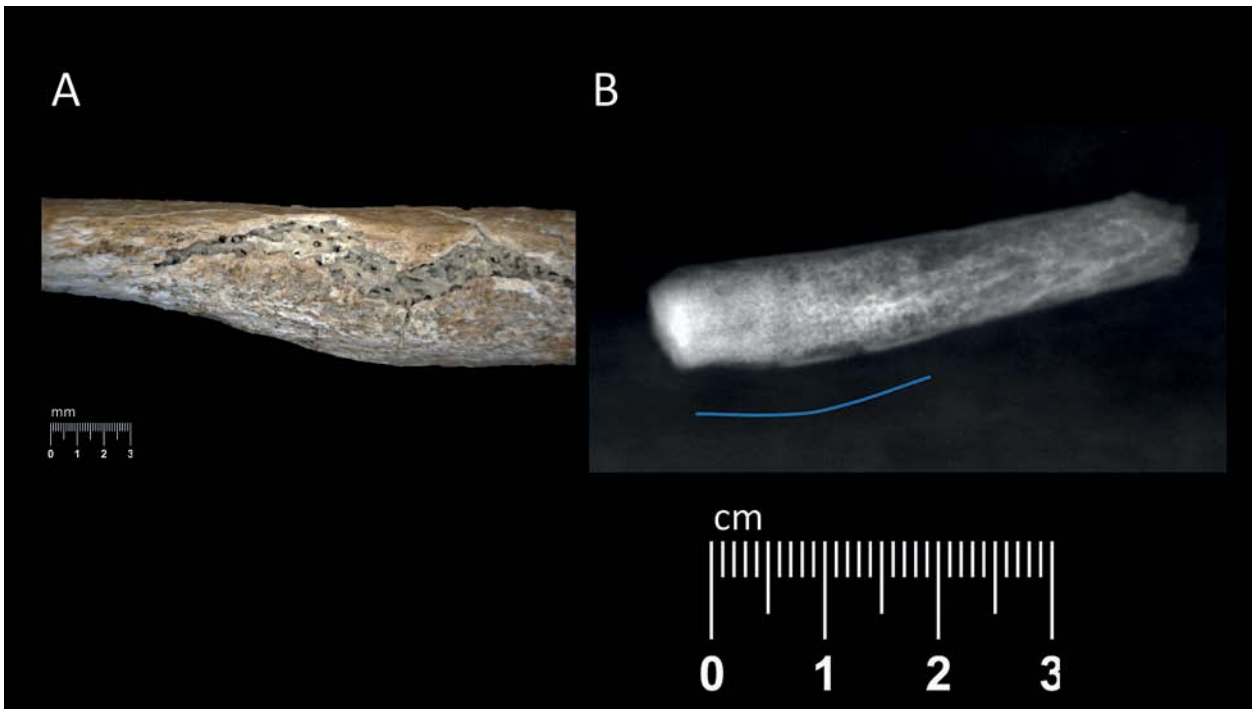

Fig. 9. (A) Superior view of the hypertrophic sternal end of a mid-rib viewed with digital microscopy. Post mortem cracking along the shaft allows direct evaluation of the hypertrophic trabeculae. **(B)** Radiopacity of the affected area (designated with a blue line) and coarsened trabeculae.

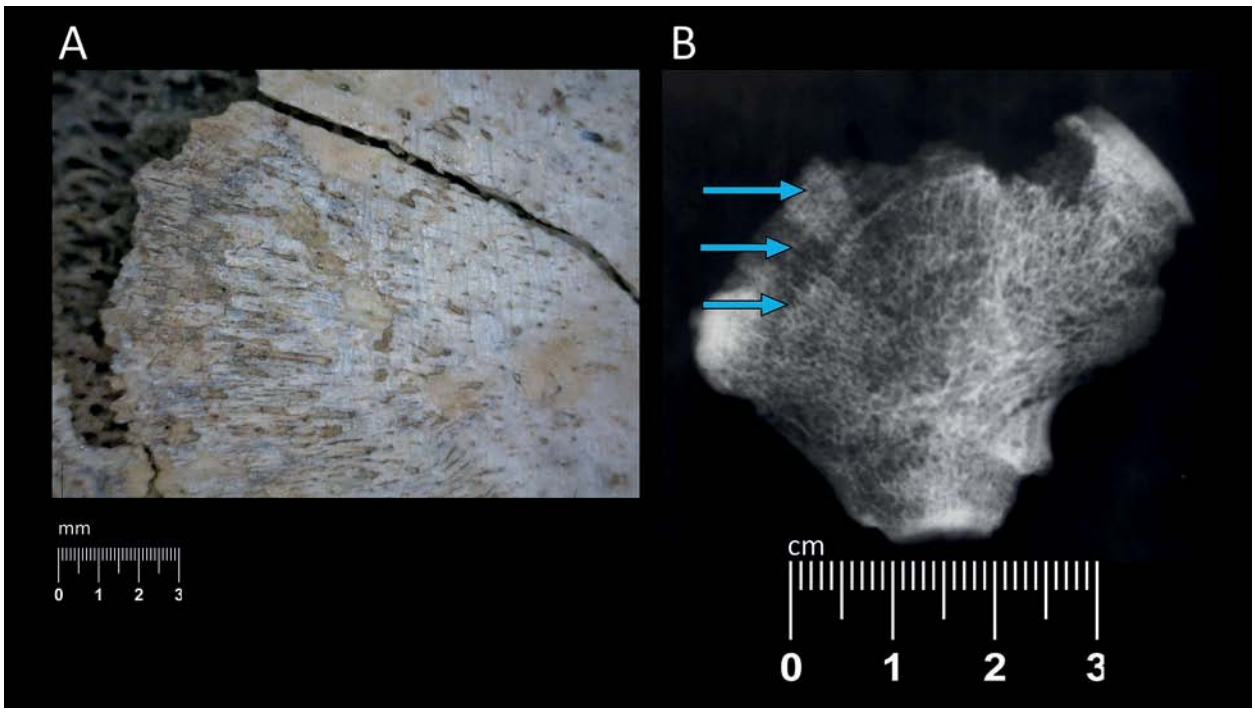

Fig. 10. (A) New bone deposition on the visceral surface of the right ilium viewed with digital microscopy. **(B)** At least three radiopaque lines that follow the contour of the iliac crest are visible radiographically together with accentuated (coarse) trabeculae throughout.

Fig. 11. Macroscopic (A) and radiographic (B) view of the humeri showing widened proximal and distal metaphyses and coarsened trabeculae.

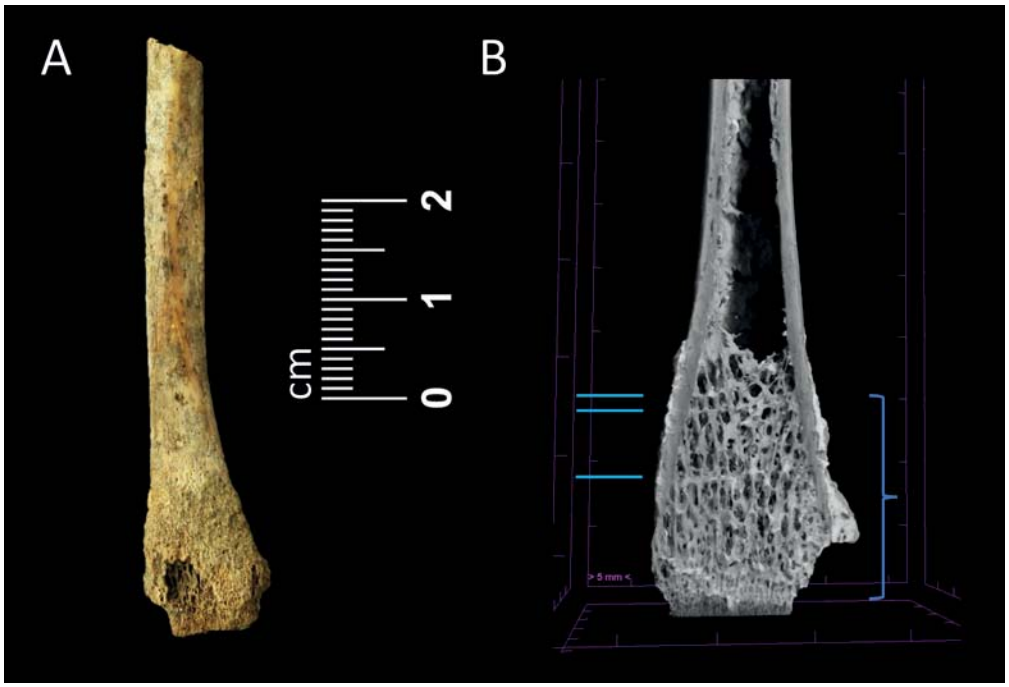

Fig. 12. Macroscopic **(A)** and micro-CT **(B)** image of the distal metaphysis of the right radius showing metaphyseal widening and distinct layers of radiodense lines and bands (bracket) close to the growth plate.

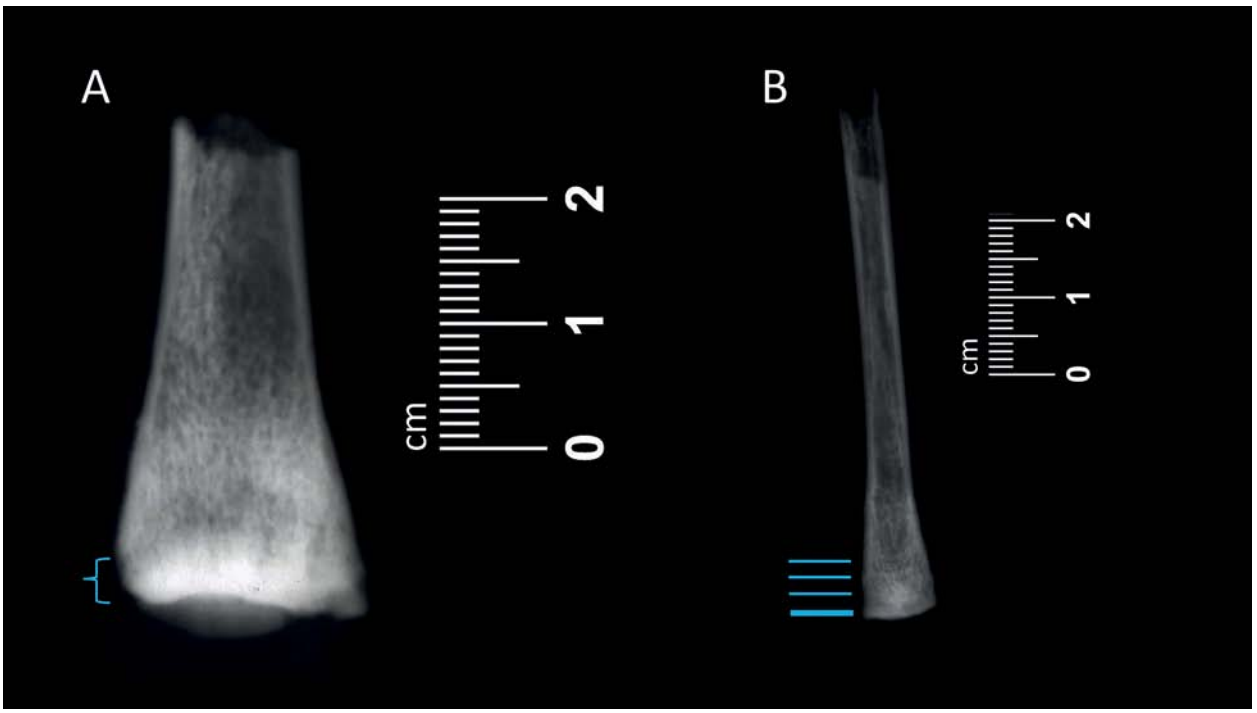

Fig. 13. **(A)** Radiograph of the distal metaphysis of the left tibia shows a thick radiopaque band adjacent to the growth plate (indicated by a bracket). **(B)** Radiograph of the distal metaphysis of the left fibula reveals a thin band adjacent to the growth plate and transverse lines visible higher up (indicated by thin lines).

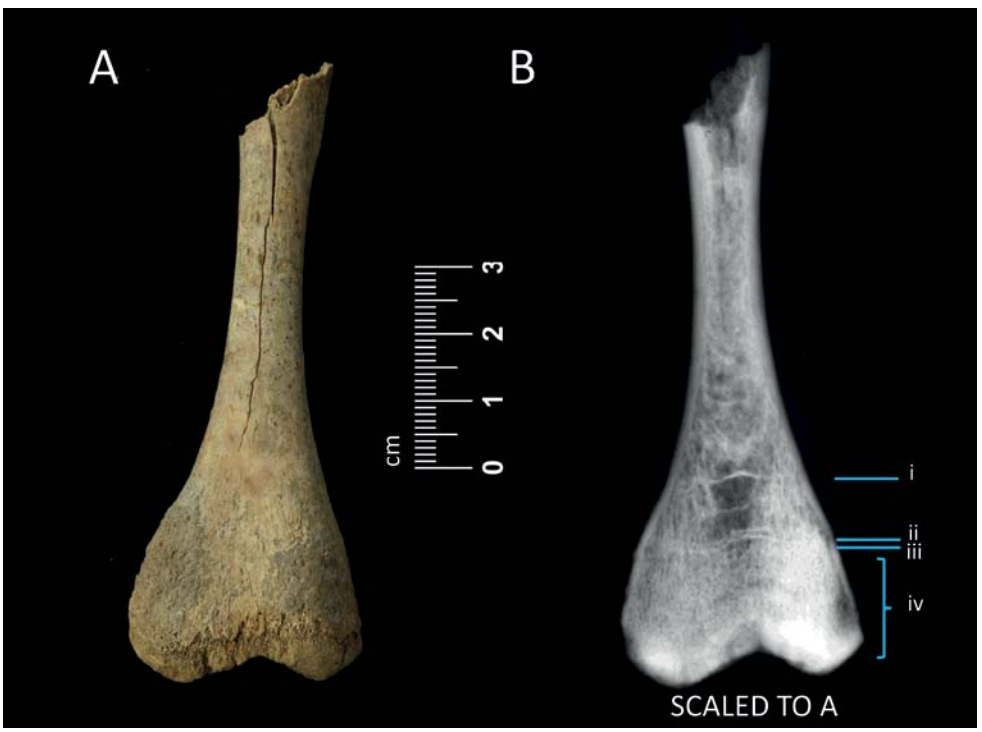

Fig. 14. Part of the diaphysis and distal metaphysis of the left femur viewed **(A)** macroscopically and **(B)** radiographically. At least three transverse radiopaque lines (i–iii) and a band of increased density (iv) following the contour of the growth plate are visible radiographically. The dense band (iv) near the growth plate measures approximately 20 mm in thickness. A thin radiopaque line (iii) is located ca. 21 mm from the growth plate, closely followed by a transverse line at ca. 22 mm (ii) from the growth plate. At around 31 mm from the growth plate, another dense line is observed (i), likely representing the earliest occurrence of the lesions.

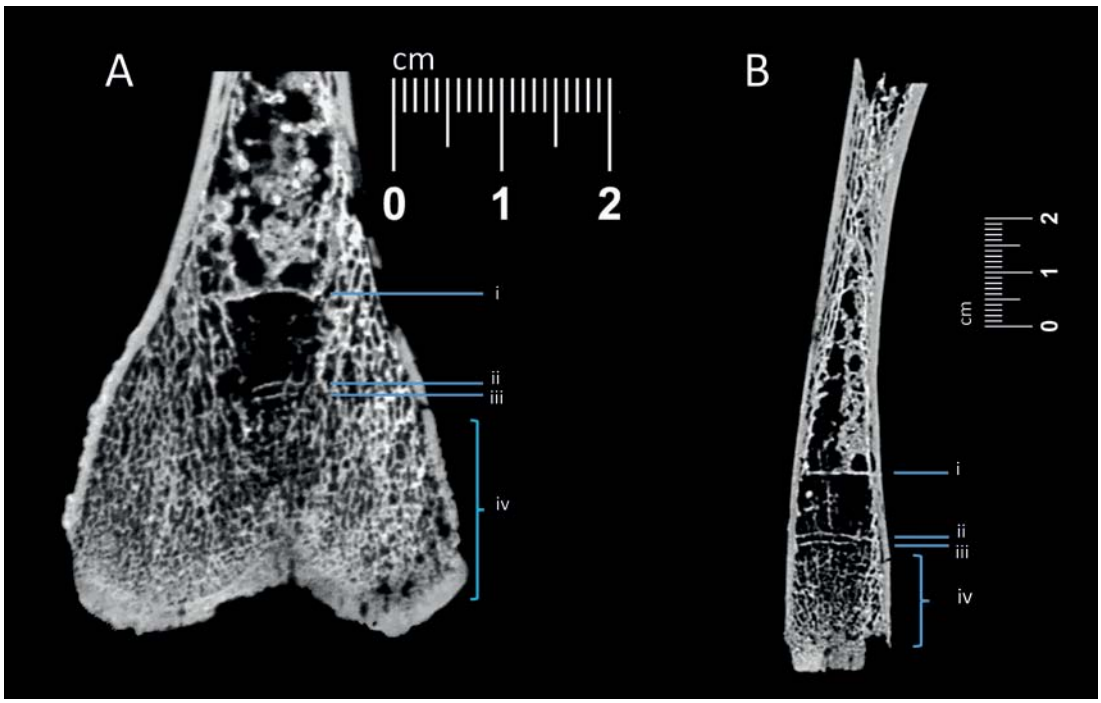

Fig. 15. Micro-CT image of the distal metaphyseal and diaphyseal areas of the left femur. **(A)** Layers of transversely oriented trabeculae (iv) extend from the growth plate towards the shaft up to approximately 20 mm. **(B)** Besides the layers of trabeculae, at least three transverse lines are visible and correspond to radiographic lines i, ii, and iii in Fig. 14B.

(Fig. 11), the proximal left ulna, the right distal radius (Fig. 12), both proximal and distal tibiae (Fig. 13A), the distal left fibula (Fig. 13B), the proximal right femur, and the distal left femur (Fig. 14 and Fig. 15).

Thick radiopaque metaphyseal bands (or 'lead lines', Resnick 1995, p. 3355; Lewis 2018, p. 272) are located adjacent to the growth plates tracing their contours. They are present at the distal radius (Fig. 12), distal femur (Fig. 14 and Fig. 15), and distal tibia (Fig. 13). The thickest band is found at the distal femur followed by the distal tibia and narrower bands are also noted at the distal left fibula and distal right radius. Bands are absent from the distal metaphyses of the humeri and most likely the proximal metaphyses of the ulnae based on the preserved elements.

At the distal metaphysis of the left tibia, a dense metaphyseal band is present (Fig. 13A). In contrast, a much narrower band is present at the distal metaphysis of the left fibula close to the growth plate, while several transverse dense lines appear at higher levels towards the shaft (Fig. 13B).

Transverse radiopaque metaphyseal lines are observed radiographically at the distal right radius, distal left femur (Fig. 14B), and distal left fibula (Fig. 13B). They are absent from the distal humeri (Fig. 11) and the left tibia (Fig. 13A).

The micro-CT images of the left femur and right radius reveal layers of transversely oriented orderly arranged trabeculae extending along the metaphysis from the growth plate towards the diaphysis (Fig. 12B, Fig. 15A and 15B). The image of the femur reveals a broader zone of rows of trabeculae that extend along the dense band (iv) visible radiographically in Fig. 14B.

4 Discussion

4.1 Differential diagnosis

Table 1 summarizes the bone lesions observed macroscopically and radiographically in the human remains from grave 23 at Thorikos. To better understand their aetiology, a differential diagnosis is conducted, and the potential impact of co-occurring pathologies on the manifestation of lesions is discussed.

4.1.1 Scurvy

Scurvy is a condition caused by a lack of sufficient vitamin C. It commonly affects individuals who suffer from nutritional deficiencies and lack important micronutrients, often also including folate and iron (Snoddy et al. 2018, p. 877). Skeletal signs of scurvy are characterized by several features throughout the skeleton, most of which are caused by episodes of hemorrhage. Since no single lesion is pathognomonic for scurvy (Brickley et al. 2020, p. 52), multiple diagnostic features are needed in a single individual to be

Table 1. Macroscopic and radiographic lesions in Tho-23 and their location.

Lesion location	Bone hyperplasia and hypertrophy	Abnormal Porosity	Endocranial irregularities	Subperiosteal new bone formation	Accentuated (coarse) trabeculae	Transverse lines of increased density	Thick radiopaque metaphyseal bands
Frontal, superolateral to orbits*	Focal hyperplasia plus thinning of outer table						
Parietal*	Focal hyperplasia: two layers of bone plus thinning of outer table	X					
Temporal: squamous part (bilateral)			X				
Occipital: lateral part (left)			X				
Sphenoid (left): foramen rotundum		X		X			
Zygomatic bones (bilateral)	Overall hypertrophy	X		X	X		
Mandible (right): medially below coronoid process		X			X		
Mandible (right): condyle	Condylar hypertrophy				X		
Ribs sternal ends	Sternal end hypertrophy	pleural side			X		
Ilium (right)	Overall hypertrophy	X		X	X	X	
Humerus Left (distal metaphysis)	Metaphyseal hypertrophy				X		
Humerus Right (proximal metaphysis* - distal metaphysis)	Metaphyseal hypertrophy						
Radius Left: (distal metaphysis*)	Metaphyseal hypertrophy						
Radius Right (distal metaphysis)	Metaphyseal hypertrophy	concave side			X	X	X
Ulna Left (proximal metaphysis*)	Metaphyseal hypertrophy				X		
Femur Left (distal metaphysis)	Metaphyseal hypertrophy	concave side			X	X	X
Femur Right (proximal metaphysis*)	Metaphyseal hypertrophy						
Tibia Left (distal metaphysis)	Metaphyseal hypertrophy				X		X
Tibia Right (proximal and distal metaphyses*)	Metaphyseal hypertrophy						
Fibula Left (distal metaphysis)	Metaphyseal hypertrophy				X	X	X

Note. Asterisk (*) designates partial skeletal preservation.

classified as probable scurvy. For a possible scurvy classification, at least one diagnostic and several suggestive features are required (Snoddy et al. 2018, p. 880).

The skeleton of Tho-23 displays at least two diagnostic and two suggestive lesions for scurvy. While lesions on both zygomatic bones are observable, the incomplete preservation of the skeleton limits the assessment of lesions bilaterally. According to Snoddy et al. (2018, table 1), the porosity and subperiosteal new bone formation at the left foramen rotundum of the sphenoid and porosity below the coronoid process of the left hemimandible are diagnostic for scurvy. Additionally, porosity on the lateral and posterior sides of the zygomatic bones and on the visceral side of the right ilium, along with new bone deposition, are suggestive of scurvy. These features are consistent with the core macroscopic lesions of scurvy identified by Brickley & Morgan (2023, table 1) and collectively support the classification of the infant from Tho-23 as having probable scurvy.

The radiographic features of the bones add complexity to diagnosis. The dense white lines observed along the growth plates of the right radius, left fibula, and right ilium may be attributed to vitamin C deficiency, which can result in hypomineralization and the retention "of provisional calcification at the ends of the metaphyses" (Brickley et al. 2020, p. 63; Tamura et al. 2000). These dense zones of calcification, known as the 'white line of Fraenkel' (Lewis 2018, p. 273), may appear alongside generalized osteopenia, thinning of the cortical bone, irregular and enlarged metaphyseal margin and spurs of mineralized bone at the metaphyseal edges (Chalouhi et al. 2020). They might also be associated with a radiolucent zone, referred to as the 'scurvy line' or 'Trümmerfeld zone', which indicates decreased osteoblastic activity (Brickley et al. 2020, pp. 64–65). None of these additional lesions are visible radiographically in Tho-23, though scurvy can still be present without them (Brickley et al. 2020, p. 63).

It is noteworthy that the manifestation of bone lesions can be influenced by the co-occurrence of other conditions (Brickley et al. 2020, pp. 239–247). Mild anemia is commonly recognized as a laboratory hallmark of scurvy (Brickley et al. 2020, p. 240), and rickets is known to occur alongside scurvy (Schattmann et al. 2016). Furthermore, rickets has been observed in a 3-year-old girl with lead poisoning (Caffey 1938).

4.1.2 Rickets

Rickets is due to vitamin D deficiency and can have diverse etiologies. It can be caused by lack of exposure and/or absorption of UVB radiation, nutritional deficiencies or inhibition of food absorption due to illness or cultural practices (Schattmann et al. 2016; Brickley et al. 2020). Its manifestation in a growing infant is largely influenced by the mother's vitamin stores during pregnancy and breastfeeding, as well as the presence of other diseases, such as scurvy, that can inhibit or reduce its effects. In such cases, depending on the timing and duration of the deficiency, subtle bone lesions may be observed (Schattmann et al. 2016, p. 64; Brickley et al. 2020, pp. 86, 95).

Several macroscopic and radiographic skeletal lesions are considered diagnostic for rickets (Brickley & Mays 2019). They are caused by the disturbance of chondrocytes and osteoblasts and failure of mineralization. Macroscopic lesions include porosity of the cranial vault, porosity and flaring at the costochondral junctions, and porosity, flaring, and cupping of the metaphyses of long bones, along with bending deformities of the ribs and long bones. Cranial vault thickening and porosity on the concave side of deformed long bones are indicative of healed or healing stages (Brickley et al. 2020, table 5-5). Radiographically, osteopenia, along with coarsening and thinning of the trabecular bone, are characteristics commonly associated with rickets (Brickley & Mays 2019).

In the infant from Thorikos grave 23, radiographic examination of all bones reveals coarsening and thinning of the trabeculae in addition to porosity on the concave side of the metaphyses of long bones. However, this porosity differs morphologically from the 'slit/strut' appearance typically associated with rickets (Brickley et al. 2020, fig. 5-11). Similarly, the porosity and hyperplasia at the sternal ends of mid-ribs in Tho-23 differs from the more localized flaring and porosity characteristic of rickets and scurvy (Brickley et al. 2020, fig. 5-11). In Tho-23, thickening of the distal rib shaft is caused by cancellous hypertrophy rather than poor mineralization; it is located on the pleural side of the costochondral junction and does not terminate in flaring. Although postmortem damage could contribute to the observed porosity, it is significant that the porosity in the rib-ends and on the concave side of the distal metaphysis of the left femur is present only in the hypertrophic areas. Additionally, the thickening and deformation of the mandibular condyle in Tho-23 are due to hypertrophy and are not consistent with the abnormal angulation of the ramus, as seen in rickets (Brickley et al. 2020, fig. 5-17). The lack of obvious macroscopic lesions, combined with the radiographic appearance of Tho-23, is consistent with a diagnosis of rickets co-occurring with scurvy, where scurvy dominates and obscures many of the features of rickets (Schattmann et al. 2016).

4.1.3 Anemias

Anemias are a group of disorders that result in reduced oxygen transport to tissues and can be either acquired or inherited (Grauer 2019). Acquired anemias have a variety of causes that depend on the specific context (Brickley 2024, p. 90). They are linked to various factors, including nutritional quality, dietary intake and absorption, bacterial and parasitic infections, as well as the demands of physiological processes like growth, menstruation, and childbirth (Grauer 2019). Genetic anemias, such as thalassemia and

sickle cell disease – common in the eastern Mediterranean – can lead to distinct skeletal features that can guide diagnosis (Hershkovitz et al. 1997; Lagia et al. 2007; Lewis 2012; Techataweewan et al. 2021). While no pathognomonic lesions exist for the acquired anemias, marrow hyperplasia is considered the most significant skeletal trait for their diagnosis, affecting both the cranial and postcranial skeleton (Brickley 2024). Marrow hyperplasia, however, is a common feature that is also associated with genetic anemias and can be especially prominent in thalassemia and sickle cell disease (Caffey 1937; Reynolds 1987; Silverman 1985).

Several lesions observed in the Thorikos infant are consistent with the presence of anemia in the skeleton: 1) marrow hyperplasia leading to widening of the diploic space on the frontal bone and thinning of the outer table, 2) a diploic-to-cortical bone ratio exceeding 1:2.5 in the frontal bone, 3) marrow hyperplasia of a parietal fragment leading to the deposition of a second layer of bone on its outer table, 4) vertical orientation of the trabeculae with large spaces between them in the same area; and 5) thinning (atrophy) of the outer table of the parietal fragment exhibiting hyperplasia. These features correspond to four of the five diagnostic criteria outlined by Brickley (2024, table 1) for diagnosing acquired anemia.

The diagnosis of an acquired rather than a genetic anemia in Tho-23 is supported by the lack of specific characteristics associated with thalassemia and sickle cell disease, such as dactylitis, which can develop as early as the fourth to sixth month of life (Caffey 1937; 1951; Poyton & Davey 1968; Moseley 1971; Bohrer 1987; O'Hara 1967). Additionally, in thalassemia, extensive marrow hyperplasia causes diffuse spongy and cortical osteopenia, along with widening of medullary cavities. This often reduces or eliminates the normal constriction in tubular bones, changing their overall shape (Silverman 1985; Lagia et al. 2007). None of these characteristics are present in the infant being studied.

The accentuated trabeculae seen throughout the skeleton could suggest early anemia, where the finer trabeculae are first resorbed due to pressure atrophy, causing the remaining ones to appear elongated and giving a more pronounced radiographic appearance (Brickley et al. 2020, p. 215). These have already been addressed in the section on rickets. Anemia can coexist with both rickets and scurvy (Brickley et al. 2020, pp. 240–241). The possibility that multiple conditions were present in the infant before death might explain the porosity found in a parietal fragment without accompanying diploic hyperplasia, which rules out anemia. The coexistence of scurvy, rickets, and anemia could result from poor dietary quality, impeded nutrient absorption or significant environmental factors. In the lead-polluted and harsh environment of Laurion, anemia likely had several causes. Heavy metals like lead can impair nutrient absorption in the gut (Brickley et al. 2020, p. 87, Bikle 2011; Raman et al. 2011) and contribute to anemia by interfering with hemoglobin synthesis and iron function.

4.1.4 Metaphyseal dysplasia (Pyle's disease)

Another condition that can cause flaring at the distal ends of tubular bones is metaphyseal dysplasia, also known as Pyle's disease. This rare inherited skeletal disorder is characterized by delayed development of the metaphyseal cortical bone (Pyle 1931; Heselson et al. 1979). The enlargement affects both the metaphyseal and diaphyseal segments symmetrically and extends beyond the metaphysis to involve large portions of the diaphyses of the tubular bones (Soares et al. 2016). Combined with the thinned cortices, the reduced medullary cavity, and the relatively late onset of this condition in later childhood (Lewis 2019, p. 632), it suggests that metaphyseal dysplasia is an unlikely explanation of the metaphyseal lesions observed in Tho-23.

4.1.5 Lead toxicity

Mimicking calcium lead is absorbed in the bones where it can be stored for decades (Burton 2008, p. 444; ATSDR 2020, p. 342). Approximately 94% of the total body lead is stored in adult bones compared to 73% in children (ATSDR 2020, p. 291; Barry 1975). Lead's elimination half-time in bones is very slow and can last 1–2 decades, whereas in the blood it can vary from one week to two years (ATSDR 2020, p. 278). This potential can be released by any trigger that affects bones' metabolism, such as pregnancy, illness or normal growth, increasing the lead level in the body and affecting the bones.

A hallmark of lead toxicity in bones is the formation of 'lead lines' visible radiographically (Caffey 1931; Park et al. 1933; Greengard 1966; Betts et al. 1973; Chisolm & Barltrop 1979; Woolf et al. 1990; Lewis 2018). Lead lines comprise radiodense transverse bands or lines across the metaphyses of tubular bones and "along the contours of flat and irregular bones" (Resnick 1995, p. 3353). The former originally appear adjacent to the growth plate, while the latter appear as inner rings that trace the contour of the vertebral bodies, epiphyses, carpal bones, and the iliac crest.

Lead lines are formed by impaired remodeling of endochondral bone due to lead deposition that inhibits osteoclastic but not osteoblastic remodeling. The process is likely triggered by the reduced blood flow in the metaphyses where lead is preferentially stored (Resnick 1995, p. 3356). While osteoblasts continue secreting osteoid, osteoclasts cannot resorb chondrocytes, which end up being covered by endosteal bone and form trabeculae of calcified cartilaginous cores (Resnick 1995, p. 3356). The tightly packed rows of sclerotic chondrocytes adjacent to the growth plate give radiographically the impression of a single band although they comprise rows of tightly packed lines of trabeculae that are discernible histologically (Caffey 1931, fig. 8C, 8D, 10; Park et al. 1933, figs. 5–8; Silverman 1985, fig. 4-236). They are also observed with finer radiographic techniques such as the micro-CT imaging in this study (Fig. 12B and Fig. 15). Contrary to a mistaken belief that lead is visible on X-rays, it is actually the more abundant calcium deposits that are

viewed in the metaphyseal regions (Leone 1968; Silverman 1985; Resnick 1995, p. 3356).

Over time, and if the child survives the toxic episode(s), lead bands thin out to little more than lines, becoming hard to distinguish before eventually vanishing (Park et al. 1933, p. 275). Due to remodeling, lead lines relocate into the bone diaphysis or substance of the flat or irregular bone following their individual rate of growth (Park et al. 1933; Sachs 1981). The knee region shows the fastest and most prolonged growth (Park et al. 1933, p. 266; Resnick 1995, p. 3353), especially the distal femur where bands are the thickest. Woolf et al. (1990, p. 91) note that "the occurrence of multiple lead lines suggests previous episodes of lead ingestion and a broad lead line indicates a more prolonged period of exposure".

In addition to producing dense radiographic lines, lead exposure disrupts the normal modeling of the metaphyseal regions in tubular bones, leading to widening or flaring (Pease & Newton 1962; Resnick 1995). Because the pathophysiology of metaphyseal widening in lead poisoning affects only the areas of cartilage proliferation, flaring remains confined to the metaphyseal regions and does not extend into the diaphysis. It is also not associated with osteopenia and shaft deformity seen in conditions such as thalassemia and Pyle's disease, as discussed earlier.

4.1.6 Harris or Park lines

Lead lines are most challenging to differentiate from transverse lines in bone caused by stress or growth arrest and recovery, also known as Harris or Park lines (Park 1964; Silverman 1985; Resnick 1995; Miszkiewicz 2015; Lewis 2018). These lines have a distinct pathophysiology and manifestation compared to lead lines as they are formed by the deposition of osteoid beneath the zone of proliferating cartilage (Lewis 2018, p. 271). During a growth arrest episode, chondroblasts cease proliferation, unlike in lead line formation, where successive rows of cartilage continue to develop. For Harris lines, osteoblasts keep depositing osteoid along the halted growth plate, but this is not immediately visible on radiographs. When growth resumes, osteoblasts add more osteoid, which then ossifies to create dense bone along the cartilage layer, eventually becoming visible radiographically (Lewis 2018, p. 271). Lead lines that have migrated towards the diaphysis due to remodeling, or scurvy lines in the healing stage (Lewis 2018, p. 273), are difficult to distinguish from Harris lines, which are also frequently observed in lead poisoning (Park et al. 1933, p. 269). Lead bands, however, in anatomical regions of rapid growth, such as the distal femoral shafts, have a characteristic morphology and breadth (Park et al. 1933, p. 287). This was shown in this paper too by the micro-CT imaging, which clearly reveals the consecutive rows of ossified cartilage formed by the ongoing production of cartilage during lead poisoning.

4.1.7 Other toxic metals

Poisoning from other metals such as bismuth injected to pregnant women with syphilis, and phosphorus administered as phosphorized cod liver oil to children with rickets and tuberculosis can cause similar lines to lead poisoning (Resnick 1995, p. 3360). Lewis (2018, p. 273) notes that histologically, bismuth poisoning differs from lead poisoning in osteoclast production and the resulting lesions. Phosphorus poisoning leads to lesions due to hyperemia in the metaphyseal areas and osteosclerosis, rather than chondrosclerosis (Caffey 1938; Resnick 1995, p. 3360).

4.2 Assessment

Several features on the infant remains indicate that the infant was suffering from lead toxicity and a number of metabolic conditions. The age-at-death of the infant at 2 years places it in the age range with the highest rate of growth. In this age the potential for lead absorption is at its highest. Moreover, it is also the age in which infants have started to crawl, walk, and experience their environment through hand to mouth transfer.

Bone lesions described for almost a century for plumbism (Caffey 1931; Park et al. 1933) are widespread throughout the infant's skeleton. Transverse bands of increased density near the growth plates suggest ongoing lead exposure until the end of the infant's life. These bands are often wider in regions of rapid growth, such as the knees and especially the distal femoral metaphyses (Park et al. 1933, p. 266; Resnick 1995). This pattern is also observed in the infant from Thorikos. The parallel rows of radiodense trabecular bone at the metaphyses, most distinctly visible on the micro-CT image (Fig. 12B and Fig. 15), mark the duration of exposure. If radiodense lines higher along the shaft correspond to earlier exposure episodes, it suggests that lead toxicity may have been present at birth or shortly thereafter. Lead lines have been documented in neonates as young as 2-days-old due to congenital lead contamination (Pearl & Boxt 1980).

All metaphyses exhibiting lead lines, as well as those without such evidence (e.g., the distal metaphyses of the humeri), display widening of their morphology due to bone hypertrophy (Pease & Newton 1962; Resnick 1995). While widened metaphyses can occur in conditions such as thalassemia and Pyle's disease, as discussed in differential diagnosis, they have distinct morphologies, extend beyond the metaphyseal regions and are not typically associated with thick radiodense bands. Further investigation of the Thorikos infant's remains also revealed widening at the ribs and the mandibular condyle, the latter being a previously unreported site that also forms endochondrally (Robinson et al. 2015). The location and distribution of lesions in anatomical areas formed by endochondral ossification is a key characteristic for the diagnosis of lead poisoning.

Lesions resulting from marrow hyperplasia provide diagnostic evidence of anemia in the infant remains. Diploic

hyperplasia is typically associated with anemia, even when not accompanied by porosity of the external table (Brickley 2024). It is currently unclear whether the thickening observed is due to lead exposure or poor nutrition in an infant weakened by repeated lead toxicity. Evidence of nutritional deficiencies, particularly scurvy, is evident in the remains, as shown by a range of lesions linked to vitamin C deficiency (Klaus 2014; Bourbou 2014; Brown & Ortner 2011; Ortner & Mays 1998; Brickley et al. 2020). Specifically, the formation of new bone in the foramen rotundum of the sphenoid bone has been observed in famine skeletons from 19th-century Ireland, indicating extremely harsh living conditions (Geber & Murphy 2012).

The likelihood that the infant may have suffered from, and possibly died due to, encephalopathy is supported by alterations observed in the temporal bones. Various types of endocranial lesions have been linked to hemorrhagic episodes and inflammatory reactions with different etiologies (Lewis 2004, 2018; Wysocka & Cieślik 2023). Given their location in the Thorikos infant, these lesions might suggest inflammation associated with the middle meningeal artery.

There are also subtle indicators that suggest the presence of rickets, potentially overshadowed by scurvy, which can obscure its full expression (Schattmann et al. 2016). While the co-occurrence of scurvy and rickets is well-documented in archaeological findings (Brickley et al. 2020, p. 239), the evidence of scurvy occurring alongside anemia, though expected, is still difficult to identify (Brickley et al. 2020, p. 240). The co-occurrence of lead toxicity and rickets has been clinically demonstrated in the case of a 3-year-old child who practiced pica (Caffey 1938). In this case, it was observed that rickets was dominant over lead toxicity, preventing the formation of lead lines until the rickets started to resolve. To the best of our knowledge, Tho-23 represents the first archaeological evidence of this co-occurrence, along with the concurrent presence of three metabolic conditions and lead poisoning.

5 Conclusions

This study identified lesions in an infant skeleton from the site of Thorikos at Laurion that are consistent with lead toxicity and the co-occurrence of metabolic diseases such as anemia, scurvy, and rickets. It suggests that these types of lesions could be more broadly applied to the study of osteological remains suspected of metal toxicity. The concurrent presence of multiple conditions suggests a complex disease environment. Digital microscopy, radiography, and micro-computed tomography are considered essential tools for accurate diagnosis, particularly in small-sized remains like those of an infant. This study provides the first osteological evidence of lead poisoning from the Laurion region in classical antiquity, laying the foundation for further research.

Acknowledgements: We would like to thank Dr. Eleni Andrikou, Director of the Ephorate of Antiquities of East Attica, and Prof. Roald Docter, Director of the Thorikos Excavations, for permission to study the remains from Thorikos; Dr. Takis Karkanas, director of the Wiener Laboratory, ASCSA, Dr. Dimitris Michailidis, coordinator of the Wiener Laboratory, ASCSA, for radiography and micro-CT scanning, and Zoe Chalatsi, Laboratory Assistant, the Wiener Laboratory, ASCSA, for the conservation of the remains; Lisa Steige for Fig. 7B, 11A, 12A and 14A, and Glauke Wylin for Fig. 4B.

Funding: This study has been made possible through the project 'Dying at the Margins of Athens: Burial Customs, Local Traditions, and Social Realities in the Attic deme of Thorikos (ca. 900–300 BCE)' funded by the Special Research Fund of Ghent University (BOF/24J/337).

References

Agency for Toxic Substances and Disease Registry (ATSDR). (2020). *Toxicological Profile for Lead*. U.S. Department of Health and Human Services, Public Health Service. https://www.atsdr.cdc.gov/ToxProfiles/tp13.pdf

AlQahtani, S. J., Hector, M. P., & Liversidge, H. M. (2010). Brief communication: The London atlas of human tooth development and eruption. *American Journal of Physical Anthropology, 142*(3), 481–490. https://doi.org/10.1002/ajpa.21258 PMID: 20310064

Aly, M. H., Kim, H. C., Renner, S. W., Boyarsky, A., Kosmin, M., & Paglia, D. E. (1993). Hemolytic anemia associated with lead poisoning from shotgun pellets and the response to Succimer treatment. *American Journal of Hematology, 44*(4), 280–283. https://doi.org/10.1002/ajh.2830440412 PMID: 8238001

American Academy of Pediatrics Council on Environmental Health. (2016). Prevention of Childhood Lead Toxicity. *Pediatrics, 138*(1), e20161493. https://doi.org/10.1542/peds.2016-1493

Apostolopoulos, G., & Kapetanios, A. (2021). Geophysical investigation, in a regional and local mode, at Thorikos Valley, Attica, Greece, trying to answer archaeological questions. *Archaeological Prospection, 28*(4), 435–452. https://doi.org/10.1002/arp.1814

Aufderheide, A. C., Neiman, F. D., Wittmers, L. E., Jr., & Rapp, G. (1981). Lead in bone II: Skeletal-lead content as an indicator of lifetime lead ingestion and the social correlates in an archaeological population. *American Journal of Physical Anthropology, 55*(3), 285–291. https://doi.org/10.1002/ajpa.1330550304 PMID: 7023243

Aufderheide, A. C., Angel, J. L., Kelley, J. O., Outlaw, A. C., Outlaw, M. A., Rapp, G., Jr., & Wittmers, L. E., Jr. (1985). Lead in bone III. Prediction of social correlates from skeletal lead content in four Colonial American populations (Catoctin Furnace, College Landing, Governor's Land, and Irene Mound). *American Journal of Physical Anthropology, 66*(4), 353–361. https://doi.org/10.1002/ajpa.1330660402 PMID: 3993761

Barry, P. S. I. (1975). A comparison of concentrations of lead in human tissues. *British Journal of Industrial Medicine, 32*(2), 119–139. https://doi.org/10.1136/oem.32.2.119 PMID: 1131339

Bergemann, J. (2021). Fragment of a Large 4th-Century BC Marble Grave Naiskos from the Thorikos Survey. In R. F. Docter & M.

Webster (Eds.), *Thorikos Reports and Studies XII* (pp. 151–162). Peeters.

Betts, P. R., Astley, R., & Raine, D. N. (1973). Lead intoxication in children in Birmingham. *British Medical Journal, 1*(5850), 402–406. https://doi.org/10.1136/bmj.1.5850.402 PMID: 4691065

Bikle, D. (2011). Vitamin D and bone mineral metabolism in hepatogastrointestinal diseases. In D. Feldman, J. Pike, & J. Adams (Eds.), *Vitamin D* (*Vol. I*, pp. 1299–1323). Academic Press. https://doi.org/10.1016/B978-0-12-381978-9.10069-1

Bingen, J. (1967a). L'Établissement du IXe Siècle et les Nécropoles du secteur Ouest 4. In H. F. Mussche, J. Bingen, J. De Geyter, G. Donnay, & T. Hackens (Eds.), *Thorikos II, 1964: Rapport Préliminaire sur la Deuxieme Campagne de Fouilles* (pp. 24–46). Comité des Fouilles Belges en Grèce.

Bingen, J. (1967b). L'Établissement Géométrique et la Nécropole Ouest. In H. F. Mussche, J. Bingen, J. Servais, J. De Geyter, T. Hackens, P. Spitaels, & A. Gautier (Eds.), *Thorikos III, 1965: Rapport Préliminaire sur la Troisieme Campagne de Fouilles* (pp. 31–56). Comité des Fouilles Belges en Grèce.

Bingen, J. (1969). L'Établissement Géométrique et la Nécropole Ouest. In H. F. Mussche, J. Bingen, J. Servais, R. Paepe, & G. Donnay (Eds.), *Thorikos IV, 1966/1967: Rapport Préliminaire sur la Quatrième Campagne de Fouilles* (pp. 70–119). Brussels.

Bohrer, S. P. (1987). Bone changes in the extremities in sickle cell anemia. *Seminars in Roentgenology, 22*(3), 176–185. https://doi.org/10.1016/0037-198x(87)90031-9 PMID: 3659956

Bourbou, C. (2014). Evidence of childhood scurvy in a Middle Byzantine Greek population from Crete, Greece (11th-12th centuries A.D.). *International Journal of Paleopathology, 5*, 86–94. https://doi.org/10.1016/j.ijpp.2013.12.002 PMID: 29539471

Brickley, M. B., & Mays, S. (2019). Metabolic disease. In J. Buikstra (Ed.), *Ortner's Identification of Pathological Conditions in Human Skeletal Remains* (pp. 531–566). Elsevier. https://doi.org/10.1016/B978-0-12-809738-0.00015-6

Brickley, M., Ives, R., & Mays, S. (2020). *The Bioarchaeology of Metabolic Bone Disease* (2nd ed.). Academic Press. https://doi.org/10.1016/B978-0-08-101020-4.00002-1

Brickley, M. B., & Morgan, B. (2023). Assessing diagnostic certainty for scurvy and rickets in human skeletal remains. *American Journal of Biological Anthropology, 181*(4), 637–645. https://doi.org/10.1002/ajpa.24799 PMID: 37337361

Brickley, M. B. (2024). Perspectives on anemia: Factors confounding understanding of past occurrence. *International Journal of Paleopathology, 44*, 90–104. https://doi.org/10.1016/j.ijpp.2023.12.001 PMID: 38181478

Brown, M., & Ortner, D. J. (2011). Childhood scurvy in a medieval burial from Mačvanska Mitrovica, Serbia. *International Journal of Osteoarchaeology, 21*(2), 197–207. https://doi.org/10.1002/oa.1124

Burton, J. H. (2008). Bone chemistry and trace element analysis. In M. A. Katzenberg & S. Saunders (Eds.), *The Biological Anthropology of the Human Skeleton* (pp. 443–460). John Wiley & Sons, Inc. https://doi.org/10.1002/9780470245842.ch14

Caffey, J. (1931). Clinical and experimental lead poisoning: Some roentgenologic and anatomic changes in growing bones. *Radiology, 17*(5), 957–983. https://doi.org/10.1148/17.5.957

Caffey, J. (1937). The skeletal changes in the chronic hemolytic anemias (erythroblastic anemia, sickle cell anemia and chronic hemolytic icterus). *The American Journal of Roentgenology and Radium Therapy, 37*, 293–324.

Caffey, J. (1938). Lead poisoning associated with active rickets: Report of a case with absence of lead lines in the skeleton. *A.M.A. American Journal of Diseases of Children, 55*(4), 798–806. https://doi.org/10.1001/archpedi.1938.01980100134010

Caffey, J. (1951). Cooley's erythroblastic anemia; some skeletal findings in adolescents and young adults. *The American Journal of Roentgenology and Radium Therapy, 65*(4), 547–560. PMID: 14819434

Cardoso, H. F. V., Abrantes, J., & Humphrey, L. T. (2014). Age estimation of immature human skeletal remains from the diaphyseal length of the long bones in the postnatal period. *International Journal of Legal Medicine, 128*(5), 809–824. https://doi.org/10.1007/s00414-013-0925-5 PMID: 24126574

Chalouhi, C., Nicolas, N., Vegas, N., Matczak, S., El Jurdi, H., Boddaert, N., & Abadie, V. (2020). Scurvy: A New Old Cause of Skeletal Pain in Young Children. *Frontiers in Pediatrics, 8*, 8. https://doi.org/10.3389/fped.2020.00008 PMID: 32083038

Chisolm, J. J., Jr., & Barltrop, D. (1979). Recognition and management of children with increased lead absorption. *Archives of Disease in Childhood, 54*(4), 249–262. https://doi.org/10.1136/adc.54.4.249 PMID: 110270

Clark, M., Royal, J., & Seeler, R. (1988). Interaction of iron deficiency and lead and the hematologic findings in children with severe lead poisoning. *Pediatrics, 81*(2), 247–254. https://doi.org/10.1542/peds.81.2.247 PMID: 3277157

Conophagos, C. E. (1980). *Le Laurium antique et la technique grecque de la production de l'argent*. Ekdotike Hellados.

Crosby, M. (1950). The Leases of the Laureion Mines. *Hesperia, 19*(3), 189–297. https://doi.org/10.2307/146776

Cunningham, C., Scheuer, L., & Black, S. (2016). *Developmental Juvenile Osteology* (2nd ed.). Academic Press.

Defever, L. (1990). *De fysische anthropologie van het oude Griekenland, met inbegrip van een analyse van het skeletmateriaal uit Thorikos*. Attika. [Master's Thesis, Rijksuniversiteit Gent]

Demetriades, A., Vergou, K., & Vlachoyiannis, N. (2008). *Η ρύπανση της Λαυρεωτικής χερσονήσου και του αστικού περιβάλλοντος του Λαυρίου από τα μεταλλευτικά-μεταλλουργικά απορρίμματα και οι επιπτώσεις στην υγεία του τοπικού πληθυσμού. Πρακτικά Θ' Επιστημονικής Συνάντησης ΝΑ. Αττικής: Λαύρειο Αττικής 13–16 Απριλίου 2000* (pp. 573–624). Εταιρεία Μελετών Νοτιοανατολικής Αττικής.

Docter, R. F., & Webster, M. (Eds.). (2018). *Exploring Thorikos*. Department of Archaeology, Ghent University.

Eastman, K. L., & Tortora, L. E. (2022). Lead Encephalopathy. In StatPearls. StatPearls Publishing. Retrieved January 15, 2025 from https://www.ncbi.nlm.nih.gov/books/NBK563167/#article-24126.s2

Erel, Y., Pinhasi, R., Coppa, A., Ticher, A., Tirosh, O., & Carmel, L. (2021). Lead in Archeological Human Bones Reflecting Historical Changes in Lead Production. *Environmental Science & Technology, 55*(21), 14407–14413. https://doi.org/10.1021/acs.est.1c00614 PMID: 34724791

Freeman, R. (1970). Chronic lead poisoning in children: A review of 90 children diagnosed in Sydney, 1948-1967. I. Epidemiological aspects. *The Medical Journal of Australia, 1*(13), 640–647. https://doi.org/10.5694/j.1326-5377.1970.tb116904.x PMID: 5445857

Geber, J., & Murphy, E. (2012). Scurvy in the Great Irish Famine: Evidence of vitamin C deficiency from a mid-19th century skeletal population. *American Journal of Physical Anthropology,*

148(4), 512–524. https://doi.org/10.1002/ajpa.22066 PMID: 22460661

Global Burden of Disease 2019 Risk Factors Collaborators. (2020). Global burden of 87 risk factors in 204 countries and territories, 1990–2019: a systematic analysis for the Global Burden of Disease Study 2019. *The Lancet, 396*(10258), 1223–1249. https://doi.org/10.1016/S0140-6736(20)30752-2

Grauer, A. (2019). Chapter 14 - Circulatory, Reticuloendothelial and Hematopoietic Disorders. In J. E. Buikstra (Ed.), *Ortner's Identification of Pathological Conditions in Human Skeletal Remains* (3rd ed., pp. 491–529). Elsevier; https://doi.org/10.1016/B978-0-12-809738-0.00014-4

Greengard, J. (1966). Lead Poisoning in Childhood: Signs, Symptoms, Current Therapy, Clinical Expressions. *Clinical Pediatrics, 5*(5), 269–276. https://doi.org/10.1177/000992286600500505

Hauptman, M., Bruccoleri, R., & Woolf, A. D. (2017). An Update on Childhood Lead Poisoning. *Clinical Pediatric Emergency Medicine, 18*(3), 181–192. https://doi.org/10.1016/j.cpem.2017.07.010 PMID: 29056870

Hershkovitz, I., Rothschild, B. M., Latimer, B., Dutour, O., Léonetti, G., Greenwald, C. M., … Jellema, L. M. (1997). Recognition of sickle cell anemia in skeletal remains of children. *American Journal of Physical Anthropology, 104*(2), 213–226. https://doi.org/10.1002/(SICI)1096-8644(199710)104:23.0.CO;2-Z PMID: 9386828

Heselson, N. G., Raad, M. S., Hamersma, H., Cremin, B. J., & Beighton, P. (1979). The radiological manifestations of metaphyseal dysplasia (Pyle disease). *The British Journal of Radiology, 52*(618), 431–440. https://doi.org/10.1259/0007-1285-52-618-431 PMID: 465917

James, A. A., & OShaughnessy, K. L. (2023). Environmental chemical exposures and mental health outcomes in children: A narrative review of recent literature. *Frontiers in Toxicology, 5*, 1290119. https://doi.org/10.3389/ftox.2023.1290119 PMID: 38098750

Kakavoyannis, E. (2001). The silver ore-processing workshops of the Lavrion region. *Annual of the British School at Athens, 96*, 365–380. https://doi.org/10.1017/S0068245400005335

Kapetanios, A. (2023). Ancient Laurion: Stages, phases and landscape. In F. Hulek, H. Lohmann, S. Nomicos, & A. Hauptmann (Eds.), *Laurion. Interdisciplinary Approaches to an Ancient Greek Mining Landscape. Der Anschnitt, Beiheft 50* (pp. 119–141).

Klaus, H. D. (2014). Subadult scurvy in Andean South America: Evidence of vitamin C deficiency in the late pre-Hispanic and Colonial Lambayeque Valley, Peru. *International Journal of Paleopathology, 5*, 34–45. https://doi.org/10.1016/j.ijpp.2013.09.002 PMID: 29539466

Kordas, K., Ravenscroft, J., Cao, Y., & McLean, E. V. (2018). Lead Exposure in Low and Middle-Income Countries: Perspectives and Lessons on Patterns, Injustices, Economics, and Politics. *International Journal of Environmental Research and Public Health, 15*(11), 2351. https://doi.org/10.3390/ijerph15112351 PMID: 30356019

Laffineur, R. (2010). Πολυάργυρος: Θορικός – Thorikos Rich in Silver: The prehistoric periods. In P. P. Iossif (Ed.), *All that glitters …": The Belgian Contribution to Greek Numismatics* (pp. 26–40). Belgian School at Athens.

Laffoon, J. E., Shuler, K. A., Millard, A. R., Connelly, J. N., & Schroeder, H. (2020). Isotopic evidence for anthropogenic lead exposure on a 17th/18th century Barbadian plantation. *American Journal of Physical Anthropology, 171*(3), 529–538. https://doi.org/10.1002/ajpa.23938 PMID: 31618449

Lagia, A., Eliopoulos, C., & Manolis, S. (2007). Thalassemia: Macroscopic and radiological study of a case. *International Journal of Osteoarchaeology, 17*(3), 269–285. https://doi.org/10.1002/oa.881

Lanphear, B. P., Hornung, R., Khoury, J., Yolton, K., Baghurst, P., Bellinger, D. C., … Roberts, R. (2005). Low-level environmental lead exposure and children's intellectual function: An international pooled analysis. *Environmental Health Perspectives, 113*(7), 894–899. https://doi.org/10.1289/ehp.7688 PMID: 16002379

Larsen, B., & Sánchez-Triana, E. (2023). Global health burden and cost of lead exposure in children and adults: A health impact and economic modelling analysis. *The Lancet. Planetary Health, 7*(10), e831–e840. https://doi.org/10.1016/S2542-5196(23)00166-3 PMID: 37714172

Leone, A. J., Jr. (1968). On lead lines. *The American Journal of Roentgenology, Radium Therapy, and Nuclear Medicine, 103*(1), 165–167. https://doi.org/10.2214/ajr.103.1.165 PMID: 5648938

Lewis, M. E. (2004). Endocranial lesions in non-adult skeletons: Understanding their aetiology. *International Journal of Osteoarchaeology, 14*(2), 82–97. https://doi.org/10.1002/oa.713

Lewis, M. (2012). Thalassaemia: Its diagnosis and interpretation in past skeletal populations. *International Journal of Osteoarchaeology, 22*(6), 685–693. https://doi.org/10.1002/oa.1229

Lewis, M. E. (2018). Paleopathology of Children. Identification of Pathological Conditions in the Human Skeletal Remains of Non-Adults. Academic Press.

Lewis, M. (2019). Skeletal dysplasias and related conditions. In J. E. Buikstra (Ed.), *Ortner's Identification of Pathological Conditions in Human Skeletal Remains* (3rd ed., pp. 615–637). Elsevier; https://doi.org/10.1016/B978-0-12-809738-0.00018-1

Mahaffey, K. R., Rosen, J. F., Chesney, R. W., Peeler, J. T., Smith, C. M., & DeLuca, H. F. (1982). Association between age, blood lead concentration, and serum 1,25-dihydroxycholecalciferol levels in children. *The American Journal of Clinical Nutrition, 35*(6), 1327–1331. https://doi.org/10.1093/ajcn/35.6.1327 PMID: 6896257

Maravelias, C., Hatzakis, A., Katsouyanni, K., Trichopoulos, D., Koutselinis, A., Ewers, U., & Brockhaus, A. (1989). Exposure to lead and cadmium of children living near a lead smelter at Lavrion, Greece. *The Science of the Total Environment, 84*, 61–70. https://doi.org/10.1016/0048-9697(89)90370-7 PMID: 2772625

Maravelias, C., Athanaselis, S., Poulos, L., Alevisopoulos, G., Ewers, U., & Koutselinis, A. (1994). Lead exposure of the child population in Greece. *The Science of the Total Environment, 158*(1-3), 79–83. https://doi.org/10.1016/0048-9697(94)90047-7 PMID: 7839127

Maravelias, C., Athanaselis, S., Dona, A., Chatzioanou, A., Priftis, C., & Koutselinis, A. (1998). Reduction of lead pollution in Greece during the past two decades. *Archives of Environmental Health, 53*(6), 424–426. https://doi.org/10.1080/00039899809605731 PMID: 9886162

Maresh, M. M. (1955). Linear growth of long bones of extremities from infancy through adolescence; continuing studies. *A.M.A. American Journal of Diseases of Children, 89*(6), 725–742.

https://doi.org/10.1001/archpedi.1955.02050110865010 PMID: 14375378

Millard, A., Montgomery, J., Trickett, M., & Beaumont, J. (2014). Childhood Lead Exposure in the British Isles during the Industrial Revolution. In M. K. Zuckerman (Ed.), *Modern Environments and Human Health. Revisiting the Second Epidemiologic Transition* (pp. 279–299). Wiley. https://doi.org/10.1002/9781118504338.ch15

Miszkiewicz, J. J. (2015). Histology of a Harris line in a human distal tibia. *Journal of Bone and Mineral Metabolism, 33*(4), 462–466. https://doi.org/10.1007/s00774-014-0644-0 PMID: 25762436

Moore, J., Filipek, K., Kalenderian, V., Gowland, R. L., Hamilton, E., Evans, J., & Montgomery, J. (2021). Death metal: Evidence for the impact of lead poisoning on childhood health within the Roman Empire. *International Journal of Osteoarchaeology, 31*(5), 846–856. https://doi.org/10.1002/oa.3001

Moorrees, C. F. A., Fanning, E. A., & Hunt, E. E., Jr. (1963). Age Variation of Formation Stages for Ten Permanent Teeth. *Journal of Dental Research, 42*(6), 1490–1502. https://doi.org/10.1177/00220345630420062701 PMID: 14081973

Moseley, J. E. (1971). Hematologic disorders. In T. H. Newton & D. G. Potts (Eds.), *Radiology of the Skull and the Brain* (pp. 697–715). CV Mosby Co.

Mussche, H. F. (1998). *Thorikos: A Mining Town in Ancient Attika*. Belgian School at Athens.

Mussche, H. F., Bingen, J., & Conophagos, C. (1973). *Thorikos 1969: rapport préliminaire sur la sixième campagne de fouilles*. Brussel: Comité des fouilles belges en Grèce.

Nakashima, T., Matsuno, K., Matsushita, M., & Matsushita, T. (2011). Severe lead contamination among children of samurai families in Edo period Japan. *Journal of Archaeological Science, 38*(1), 23–28. https://doi.org/10.1016/j.jas.2010.07.028

Nakos, G. (1979). Lead pollution: Fate of lead in the soil and its effects on Pinus halepensis. *Plant and Soil, 53*(4), 427–443. Retrieved from http://www.jstor.org/stable/42934982 https://doi.org/10.1007/BF02140715

Nakou, S., Mengreli, C., Karaklis, A., & Lapatsanis, P. (1980). Five siblings with chronic lead poisoning. *Pediatric Research, 14*(12), 1420. https://doi.org/10.1203/00006450-198012000-00071

Nakou, S. (1985). Επίπεδα μόλυβδου αίματος και νεφρική λειτουργία παιδιών μιας περιοχής με αυξημένο περιβαλλοντικό μόλυβδο. [Διατριβή. Ιατρική Σχολή Πανεπιστημίου Ιωαννίνων].

Nriagu, J. O. (1983). *Lead and Lead Poisoning*. John Wiley & Sons, Inc. http://hdl.handle.net/10427/010621

O'Hara, A. E. (1967). Roentgenographic osseous manifestations of the anemias and the leukemias. *Clinical Orthopaedics and Related Research, 52*(52), 63–82. https://doi.org/10.1097/00003086-196700520-00007 PMID: 5233390

Ortner, D. J., & Mays, S. (1998). Dry-bone Manifestations of Rickets in Infancy and Early Childhood. *International Journal of Osteoarchaeology, 8*(1), 45–55. https://doi.org/10.1002/(SICI)1099-1212(199801/02)8:13.0.CO;2-D

Panzer, S., Schneider, K. O., Zesch, S., Rosendahl, W., Helmbold-Doyé, H., Thompson, R. C., & Zink, A. R. (2022). Recovery lines in ancient Egyptian child mummies: Computed tomography investigations in European museums. *International Journal of Osteoarchaeology, 32*(3), 682–693. https://doi.org/10.1002/oa.3095

Park, E. A., Jackson, D., Goodwin, T. C., & Kajdi, L. (1933). X-ray shadows in growing bones produced by lead; Their characteristics, cause, anatomical counterpart in the bone and differentiation. *The Journal of Pediatrics, 3*(2), 265–298. https://doi.org/10.1016/S0022-3476(33)80110-7

Park, E. A. (1964). The imprinting of nutritional disturbances on the growing bone. *Pediatrics, 33*(5), 815–862. https://doi.org/10.1542/peds.33.5.815 PMID: 14152896

Pearl, M., & Boxt, L. M. (1980). Radiographic findings in congenital lead poisoning. *Radiology, 136*(1), 83–84. https://doi.org/10.1148/radiology.136.1.6770416 PMID: 6770416

Pease, C. N., & Newton, G. G. (1962). Metaphyseal dysplasia due to lead poisoning in children. *Radiology, 79*(2), 233–240. https://doi.org/10.1148/79.2.233 PMID: 14484793

Poyton, H. G., & Davey, K. W. (1968). Thalassemia. Changes visible in radiographs used in dentistry. *Oral Surgery, Oral Medicine, and Oral Pathology, 25*(4), 564–576. https://doi.org/10.1016/0030-4220(68)90301-0 PMID: 5238794

Pyle, E. (1931). A Case of unusual bone development. *The Journal of Bone & Joint Surgery, 13*(4), 874–876.

Raman, M., Milestone, A. N., Walters, J. R., Hart, A. L., & Ghosh, S. (2011). Vitamin D and gastrointestinal diseases: Inflammatory bowel disease and colorectal cancer. *Therapeutic Advances in Gastroenterology, 4*(1), 49–62. https://doi.org/10.1177/1756283X10377820 PMID: 21317994

Rasmussen, K. L., Skytte, L., Jensen, A. L., & Boldsen, J. L. (2015). Comparison of mercury and lead levels in the bones of rural and urban populations in Southern Denmark and Northern Germany during the Middle Ages. *Journal of Archaeological Science, Reports, 3*, 358–370. https://doi.org/10.1016/j.jasrep.2015.06.021

Resnick, D. (1995). *Diagnosis of Bone and Joint Disorders*. W.B. Saunders Company.

Reynolds, J. (1987). The skull and spine. *Seminars in Roentgenology, 22*(3), 168–175. https://doi.org/10.1016/0037-198X(87)90030-7 PMID: 3659955

Robinson, J., O'Brien, A., Chen, J., & Wadhwa, S. (2015). Progenitor Cells of the Mandibular Condylar Cartilage. *Current Molecular Biology Reports, 1*(3), 110–114. https://doi.org/10.1007/s40610-015-0019-x PMID: 26500836

Rosen, J. F., Chesney, R. W., Hamstra, A., DeLuca, H. F., & Mahaffey, K. R. (1980). Reduction in 1,25-dihydroxyvitamin D in children with increased lead absorption. *The New England Journal of Medicine, 302*(20), 1128–1131. https://doi.org/10.1056/NEJM198005153022006 PMID: 7366636

Ross, J., Voudouris, P., Melfos, V., Vaxevanopoulos, M., Soukis, K., & Merigot, K. (2021). The Lavrion silver district: Reassessing its ancient mining history. *Geoarchaeology, 36*(4), 617–642. https://doi.org/10.1002/gea.21852

Sachs, H. K. (1981). The evolution of the radiologic lead line. *Radiology, 139*(1), 81–85. https://doi.org/10.1148/radiology.139.1.7208946 PMID: 7208946

Salliora-Oikonomakou, M. (1985). Αρχαίο νεκροταφείο στην περιοχή Λαυρίου. *Archaiologikon Deltion, 40*(A), 90–132.

Schattmann, A., Bertrand, B., Vatteoni, S., & Brickley, M. (2016). Approaches to co-occurrence: Scurvy and rickets in infants and young children of 16-18th century Douai, France. *International Journal of Paleopathology, 12*, 63–75. https://doi.org/10.1016/j.ijpp.2015.12.002 PMID: 29539522

Schroeder, H., Shuler, K. A., & Chenery, S. R. (2013). Childhood lead exposure in an enslaved African community in Barbados: Implications for birthplace and health status. *American Journal of Physical Anthropology, 150*(2), 203–209. https://doi.org/10.1002/ajpa.22193 PMID: 23225156

Silverman, F. N. (1985). *Caffey's Pediatric X-ray Diagnosis. An integrated Imaging Approach* (*Vol. 1*). Yearbook Medical Publishers.

Skarpelis, N., & Argyraki, A. (2009). Geology and origin of supergene ore at the Lavrion Pb-Ag-Zn deposit, Attica, Greece. *Resource Geology, 59*(1), 1–14. https://doi.org/10.1111/j.1751-3928.2008.00076.x

Snoddy, A. M. E., Buckley, H. R., Elliott, G. E., Standen, V. G., Arriaza, B. T., & Halcrow, S. E. (2018). Macroscopic features of scurvy in human skeletal remains: A literature synthesis and diagnostic guide. *American Journal of Physical Anthropology, 167*(4), 876–895. https://doi.org/10.1002/ajpa.23699 PMID: 30298514

Soares, D. X., Almeida, A. M., Barreto, A. R. F., Alencar E Silva, I. J., de Castro, J. D. V., Magalhães Pinto, F. J., … Aguiar, L. B. (2016). Pyle disease (metaphyseal dysplasia) presenting in two adult sisters. *Radiology Case Reports, 11*(4), 405–410. https://doi.org/10.1016/j.radcr.2016.10.003 PMID: 27920870

Tamura, Y., Welch, D. C., Zic, J. A., Cooper, W. O., Stein, S. M., & Hummell, D. S. (2000). Scurvy presenting as painful gait with bruising in a young boy. *Archives of Pediatrics & Adolescent Medicine, 154*(7), 732–735. https://doi.org/10.1001/archpedi.154.7.732 PMID: 10891027

Techataweewan, N., Mann, R. W., Vlok, M., Ruengdit, S., Panthongviriyakul, C., & Buckley, H. R. (2021). Thalassemia major in a 49-year-old Thai female: Gross and X-ray examination of dry bone. *International Journal of Osteoarchaeology, 31*(5), 866–880. https://doi.org/10.1002/oa.3003

U.S. Environmental Protection Agency. (2022). *Strategy to Reduce Lead Exposures and Disparities in U.S. Communities*. Environmental Protection Agency. https://www.epa.gov/system/files/documents/2022-11/Lead%20Strategy_1.pdf

Valentine, W. N., Paglia, D. E., Fink, K., & Madokoro, G. (1976). Lead poisoning: Association with hemolytic anemia, basophilic stippling, erythrocyte pyrimidine 5′-nucleotidase deficiency, and intraerythrocytic accumulation of pyrimidines. *The Journal of Clinical Investigation, 58*(4), 926–932. https://doi.org/10.1172/JCI108545 PMID: 965496

von Lindern, I., Spalinger, S., Stifelman, M. L., Stanek, L. W., & Bartrem, C. (2016). Estimating Children's Soil/Dust Ingestion Rates through Retrospective Analyses of Blood Lead Biomonitoring from the Bunker Hill Superfund Site in Idaho. *Environmental Health Perspectives, 124*(9), 1462–1470. https://doi.org/10.1289/ehp.1510144 PMID: 26745545

Voudouris, P., Melfos, V., Mavrogonatos, C., Photiades, A., Moraiti, E., Rieck, B., … Zaimis, S. (2021). The Lavrion Mines: A Unique Site of Geological and Mineralogical Heritage. *Minerals (Basel), 11*(1), 76. https://doi.org/10.3390/min11010076

Wani, A. L., Ara, A., & Usmani, J. A. (2015). Lead toxicity: A review. In *Interdisciplinary Toxicology* (Vol. 8, Issue 2, pp. 55–64). Slovak Toxicology Society. https://doi.org/10.1515/intox-2015-0009

Woolf, D. A., Riach, I. C., Derweesh, A., & Vyas, H. (1990). Lead lines in young infants with acute lead encephalopathy: A reliable diagnostic test. *Journal of Tropical Pediatrics, 36*(2), 90–93. Retrieved from https://academic.oup.com/tropej/article/36/2/90/1668583 https://doi.org/10.1093/tropej/36.2.90 PMID: 2355410

Wright, R. O., Shannon, M. W., Wright, R. J., & Hu, H. (1999). Association between iron deficiency and low-level lead poisoning in an urban primary care clinic. *American Journal of Public Health, 89*(7), 1049–1053. https://doi.org/10.2105/AJPH.89.7.1049 PMID: 10394314

Wysocka, J., & Cieślik, A. (2023). The frequency and macromorphological classification of abnormal blood vessel impressions and periosteal appositions of the dura mater in an early modern osteological collection from Poland. *International Journal of Paleopathology, 41*, 78–87. https://doi.org/10.1016/j.ijpp.2023.04.001 PMID: 37031588

Xenophon. (2013). Memorabilia (E. C. Marchant, O. J. Todd, & J. Henderson, Trans). Harvard University Press. https://doi.org/10.4159/DLCL.xenophon_athens-memorablia_2013.2013

Zhou, N., Huang, Y., Li, M., Zhou, L., & Jin, H. (2022). Trends in global burden of diseases attributable to lead exposure in 204 countries and territories from 1990 to 2019. *Frontiers in Public Health, 10*, 1036398. https://doi.org/10.3389/fpubh.2022.1036398 PMID: 36504990

Manuscript received: August 26, 2024
Revisions requested: December 13, 2024
Revised version received: February 7, 2025
Manuscript accepted: February 18, 2025